AD-A109 947 SCIENCE APPLICATIONS INC MCLEAN VA F/G 20/4
FLUID DYNAMICS-REACTIVE FLOW MODELING.(U)
DEC 81 E HYMAN, M FRY, J TITTSWORTH, D FYFE N00014-81-C-2085
UNCLASSIFIED SAI-82-655-WA NL

END
DATE FILMED
3 82
DTIC

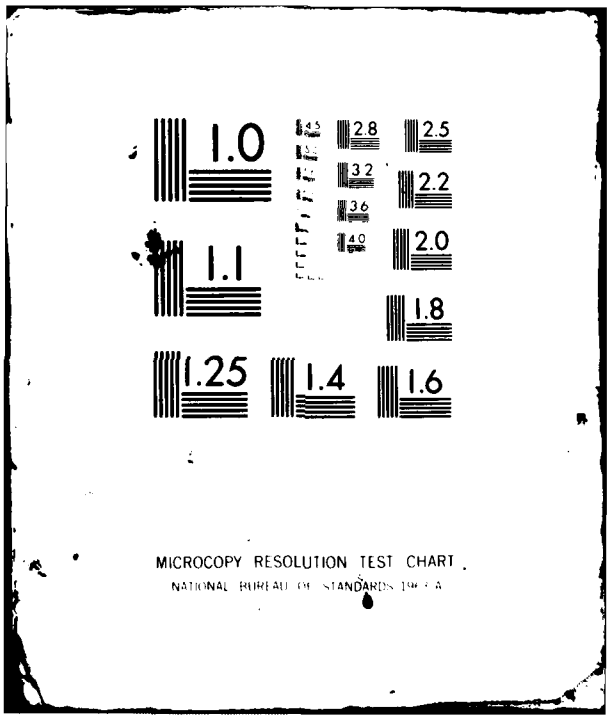
1.0
1.1
1.25
1.4
1.6
1.8
2.0
2.2
2.5
2.8
3.2
3.6
4.0
MICROCOPY RESOLUTION TEST CHART
NATIONAL BUREAU OF STANDARDS 1963-A

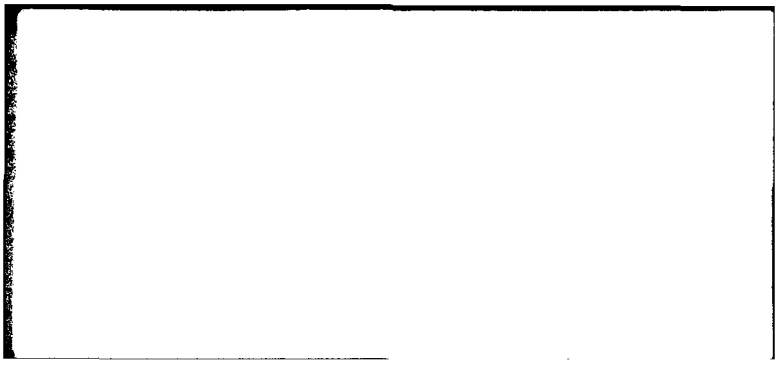

DISCLAIMER NOTICE

THIS DOCUMENT IS BEST QUALITY PRACTICABLE. THE COPY FURNISHED TO DTIC CONTAINED A SIGNIFICANT NUMBER OF PAGES WHICH DO NOT REPRODUCE LEGIBLY.

FLUID DYNAMICS-REACTIVE FLOW MODELING

Final Report

SAI-82-655-WA

16 Dec 1981

FLUID DYNAMICS-REACTIVE FLOW MODELING

Final Report

SAI-82-655-WA

Submitted to:

Laboratory for Computational Physics
Code 4040
Naval Research Laboratory
Washington, D.C. 20375

Prepared Under:

Contract #N00014-81-C-2085

Prepared by:

Ellis Hyman

with

Mark Fry
Jeff Tittsworth
David Fyfe
K. Kailasanath

SCIENCE APPLICATIONS, INC.

P.O. Box 1303
1710 Goodridge Drive
McLean, Virginia 22102

(703) 734-5840

TABLE OF CONTENTS

GENERAL DISCUSSION

In the following discussion we will describe the work performed by Science Applications, Inc. (SAI) on contract number N00014-81-C-2085, SAI project number 1-157-18-265, entitled "Fluid Dynamics-Reactive Flow Modeling," which had a technical performance period of 1 December 1980 to 30 November 1981.

This work includes (1) adaptations of the FAST2D code for slow flow applications, (2) use of the FAST2D code to model vorticity and turbulence flow efficiently, (3) an analytical and computational study of the ignition and quenching of laminar flames in a premixed H_2, O_2, N_2 mixture, and (4) incorporation of the latest reactive flow computer packages into the NRL ionosphere code. Each of these topics will be described in the following paragraphs.

SAI has recently increased the flexibility and efficiency of FAST2D, a two dimensional hydrocode developed by The Laboratory for Computational Physics at NRL. The transport algorithm used for transporting density, momentum, energy, and chemical species has been altered to compute along as many as ten rows of computational cells at a time. The original algorithm could only accommodate one row at a time. The new algorithm was compared to the original using a cylindrical axisymmetric shear flow problem. Since no changes were made in the differencing scheme itself, the new algorithm gave exactly the same results as the original. A factor of five increase in computing speed was obtained.

In preparation for reactive slow flow modeling FAST2D's mechanism for following chemical species was altered. Number densities rather than fractional densities for all the species are transported in order to make FAST2D compatible with existing chemical reaction schemes and molecular diffusion packages. The revised version has been benchmarked in a non-reacting shear-flow problem similar to the one mentioned above. As a result, no significant numerical diffusion of chemical species occurred.

A project involving shock modeling was also completed using FAST2D. The object of the study was to accurately and efficiently capture the various structures in complex, non-steady shocks. The quasi-Lagrangian rezoning capabilities of FAST2D were sufficient for modeling two of the four cases studied, regular and single mach reflection. Complex and double mach reflections were modeled after an additional rezoning capability was added to FAST2D. The code was modified to allow the grid to expand about any arbitrary point within the computational system. In this way, grid and fluid motions were synchronized such that self-similar shock structures could grow naturally with the system. This work has been reported in Fry, M., et al., "Shock Capturing Using Flux-Corrected Transport Algorithms with Adaptive Gridding," NRL Memo Report 4629 (1981) and appears in this report as Appendix A. This new adaptive gridding technique allows one to more efficiently model vorticity and turbulence flows.

A theoretical and computational study of the ignition and quenching of laminar flames in a premixed H_2:O_2:N_2 mixture has been performed and a detailed report of the work, entitled "A Theoretical Study of the Ignition of Pre-Mixed Gases," is included as Appendix B. The objectives

of this work were: (1) to complete the calibration of the similarity solution model, and (2) to utilize the similarity solution model in conjunction with the NRL 1-D flame model to study the ignition, propagation and quenching of laminar flames in premixed gases.

The similarity solution model is based on an analytic similarity solution to the non-linear time-dependent slow flow equations. The similarity solution and the induction time for the fuel-oxidizer mixture as a function of temperature and pressure can be used to calculate whether or not a given energy source is adequate to ignite the system. This simple procedure is then calibrated using the NRL 1-D flame model which includes the thermophysical properties of the mixture, a full chemical kinetics scheme, nonlinear convection, molecular diffusion and thermal conduction. The details of the calibration are given in Appendix B.

The similarity solution model predicts whether or not a mixture will ignite given the initial radius of energy deposition R_o, the duration of the heating τ_o and the total energy deposited in the system E_o. If ignition is predicted, the model gives the time it takes for ignition to occur. In contrast, the NRL flame model not only predicts ignition, but also provides the structure of the propagating flame. The calculations presented in Appendix B show that the similarity solution predicts ignition accurately when the radius of energy deposition is larger than the quench radius. The NRL flame model is used to estimate the quench radius as well as to explain the discrepancy in the predictions of the two models for very small radii of energy deposition.

SAI has incorporated the latest reactive flow computer packages into the NRL computer code for the

numerical modeling of the mid-latitude ionosphere.[1] There are two significant additions to the code to improve speed and flexibility. Firstly, the ordinary differential equation (ODE) solver, IMPLCT, used to time advance the chemistry part of the continuity equations was replaced by one which takes advantage of the form of the equations. If there are NZ grid points in altitude, then the ODE's decouple into NZ systems since with the time-splitting algorithm used the chemistry at a given altitude will not depend on the chemistry at any other altitude within the one hydrodynamic time step. Doing many systems at once is an ideal situation for a vector computer like the TI-ASC. The computer package, VSAIM, developed at NRL does such a problem. Since the chemistry at one altitude may proceed faster than at another altitude, VSAIM allows each system to use its own time step. After each chemistry time step it terminates those that have reached the desired ending time and if necessary starts a new system thus keeping the vectors as optimally long as possible throughout the computation. VSAIM, like its predecessor, CHEMEQ,[2] also tries to treat those equations it deems are difficult to solve with a special algorithm for stiff equations and those which are easy to solve with a simpler algorithm.

The second major incorporation into the 1D ionosphere code is a routine for the processing of chemical reactions and their reaction rates. Formerly these reactions and reaction rates were hard-wired with the program, requiring program modification for even the slightest change in reaction rate coefficients or the number of reactions. By using the automatic rate processor, ARTP, the chemical reactions and their corresponding reaction rates are input as data cards allowing great flexibility in the choice of the type of chemistry one elects to incorporate into the ionospheric model.

In order to make these modifications it was necessary to change the data structures used to store the densities of the various chemical species. Instead of using a distinct array for each specie present in the problem, one larger array indexed by the number of species in the problem is now used. An array of symbols is now used to distinguish one specie from another. These symbols are the data that ARTP uses to recognize which species are involved in each reaction it processes. By making the types of ions and minor neutrals input to the program, the user has a greater flexibility to test the effects of various chemical reactions and the importance of the various ions or minor neutrals on the resulting ionosphere.

While the modifications to the code were being made, documentation describing the variables used by the code was added. Furthermore, a separate piece of documentation was added to describe the input data to the program, making the whole program much more user oriented. In Appendix C we have included the revised versions of 2 subroutines - INITAL and RTCON. These subroutines supply all the information necessary for setting up the input required for making a run of the ionosphere code.

REFERENCES

1. E. S. Oran, T. R. Young, Jr., D. V. Anderson, T. P. Coffey, P. C. Kepple, A. W. Ali, and D. F. Strobel, "A Numerical Model of the Mid-Latitude Ionosphere," NRL Memorandum Report 2839, July 1974.

2. T. R. Young, "CHEMEQ - A Subroutine for Solving Stiff Ordinary Differential Equations," NRL Memorandum Report 4091, February 26, 1980.

Appendix A

SHOCK CAPTURING USING FLUX-CORRECTED TRANSPORT ALGORITHMS WITH ADAPTIVE GRIDDING

SHOCK CAPTURING USING FLUX-CORRECTED TRANSPORT ALGORITHMS WITH ADAPTIVE GRIDDING

M. Fry and J. Tittsworth
Science Applications, Inc.
McLean, Virginia, 22102, USA

A. Kuhl
R and D Associates
Marina del Rey, California, 90291, USA

D. Book, J. Boris and M. Picone
Laboratory for Computational Physics
U. S. Naval Research Laboratory
Washington, D.C., 20375, USA

A numerical technique has been developed for capturing complex, nonsteady shock structures in multidimensions. The technique relies on moving the computational mesh with the shock wave so that the features of principal interest appear approximately stationary. The method has been implemented using coordinate-split Flux-Corrected Transport (FCT) algorithms which allow the mesh to evolve arbitrarily with respect to the fluid in each coordinate. The grid may thus be optimized in response to the needs of a given problem. Synchronizing the grid and fluid motions permits significant reduction of numerical transients and eliminates numerical diffusion. Shocks develop naturally, with no fitting. The method is illustrated by calculating complex, two-dimensional Mach reflection phenomena associated with airblasts and shock diffraction on wedges. The numerical results are in good agreement with available experimental data.

INTRODUCTION

Numerical solution of transient multidimensional gas dynamics problems is always nontrivial. When, in addition, the problem involves reflecting supersonic flows, large variations in length scales in both space and time, or phenomena for which neither analytic solutions nor detailed experimental observations are at hand, the state of the computational art is challenged. Such a problem arises in calculating the oblique reflection of shocks from solid surfaces in planar geometries (e.g. shock tube experiments) or axisymmetric geometries (e.g. airblasts). The complications arise mainly from the presence of Mach reflections which occur when a shock front impinges on a reflecting surface at angles of incidence sufficiently far from normal. The formation of a Mach stem and, consequently, of a slip surface intersecting the triple point (the confluence of the incident, Mach, and reflected waves) results from the requirement that the flow behind the reflected shock be parallel to the reflecting surface, which cannot be achieved through regular reflection.

Attempts to calculate the properties of the flow in Mach reflections date back at least to von Neumann[1] and the research which grew out of the wartime explosive studies[2-4]. For the simplest problem, that of a planar shock

Manuscript submitted August 24, 1981.

reflecting from a plane surface, Jones, Martin, and Thornhill[5] noted that it is possible to reduce the number of independent variables to two by transforming to the similarity variables x/t, y/t, a device that was also used by Kutler, et al[6]. Ben-Dor[7] developed a theory which used shock polars to explain some of the features of this problem, and solved the system of algebraic equations obtained by combining the jump conditions across the various discontinuities (Courant and Friedrichs)[8] to describe the flow in the neighborhood of the triple point. To date, no satisfactory treatment of the complete flow field has been published, although some features (like the shape of various waveforms) are quite easy to model.

In connection with studies of both chemical and nuclear explosions there have been many attempts to model a spherical blast wave reflecting from the ground, the so-called height-of-burst (HOB) problem. The hydrodynamic phenomena in the two cases are identical, although nonideal effects (primarily explosive afterburn in the first instance and radiation preheating in the second) are different. Previous attempts to model two-dimensional complex shock reflection have suffered from restriction to describing part of the system, the use of a special assumption like that of self-similarity, or less than satisfactory agreement with experimental data.[9]

The calculations discussed here represent a step forward in overcoming these difficulties. They differ from previous numerical work in incorporating two important computational developments: Flux-Corrected Transport (FCT)[10] and an adaptive regridding procedure, called "sliding rezone",[11] which optimizes the mesh point distribution and hence the resolution of surfaces of discontinuity.

FCT is a finite-difference technique for solving the fluid equations in problems where sharp discontinuities arise (e.g. shocks, slip surfaces and contact surfaces). It modifies the linear properties of a second- (or higher) order algorithm by adding a diffusion term during convective transport, and then subtracting it out "almost everywhere" in the antidiffusion phase of each time step. The residual diffusion is just large enough to prevent dispersive ripples from arising at the discontinuity, thus ensuring that all conserved quantities remain positive. FCT captures shocks accurately over a wide range of parameters. No information about the number or nature of the surfaces of discontinuity need be provided prior to initiating the calculation.

The FCT routine used in the present calculations, called JPBFCT (an advanced version of ETBFCT)[12], consists of a flexible, general transport module which solves 1-D fluid equations in Cartesian, cylindrical, or spherical geometry. It provides a finite difference approximation to the conservation laws of the general form:

$$\frac{\partial}{\partial t}\int_{\delta V(t)} \Phi dV = -\int_{\delta A(t)} \Phi\,(\underline{u}-\underline{u}_g)\cdot d\underline{A} + \int_{\delta A(t)} \tau dA \qquad (1)$$

where Φ represents the mass, momentum, energy or mass species in cell $\delta V(t)$, $\underline{u}$ and $\underline{u}_g$ represent the fluid and grid velocities, respectively, and τ represents the pressure/work terms. This formulation allows the grid to slide with respect to the fluid without introducing any additional numerical diffusion. Thus, knowing where the features of greatest interest are located, one can concentrate fine zones where they will resolve these features most effectively as the system evolves (Fig. 1).

In the next section we describe the computational techniques used to solve the wedge problem and present the results of four simulations carried out to reproduce experimental results of Ben-Dor and Glass.[13] In Section III we present a parallel discussion for a HOB calculation. Finally, in Section IV we summarize our conclusions.

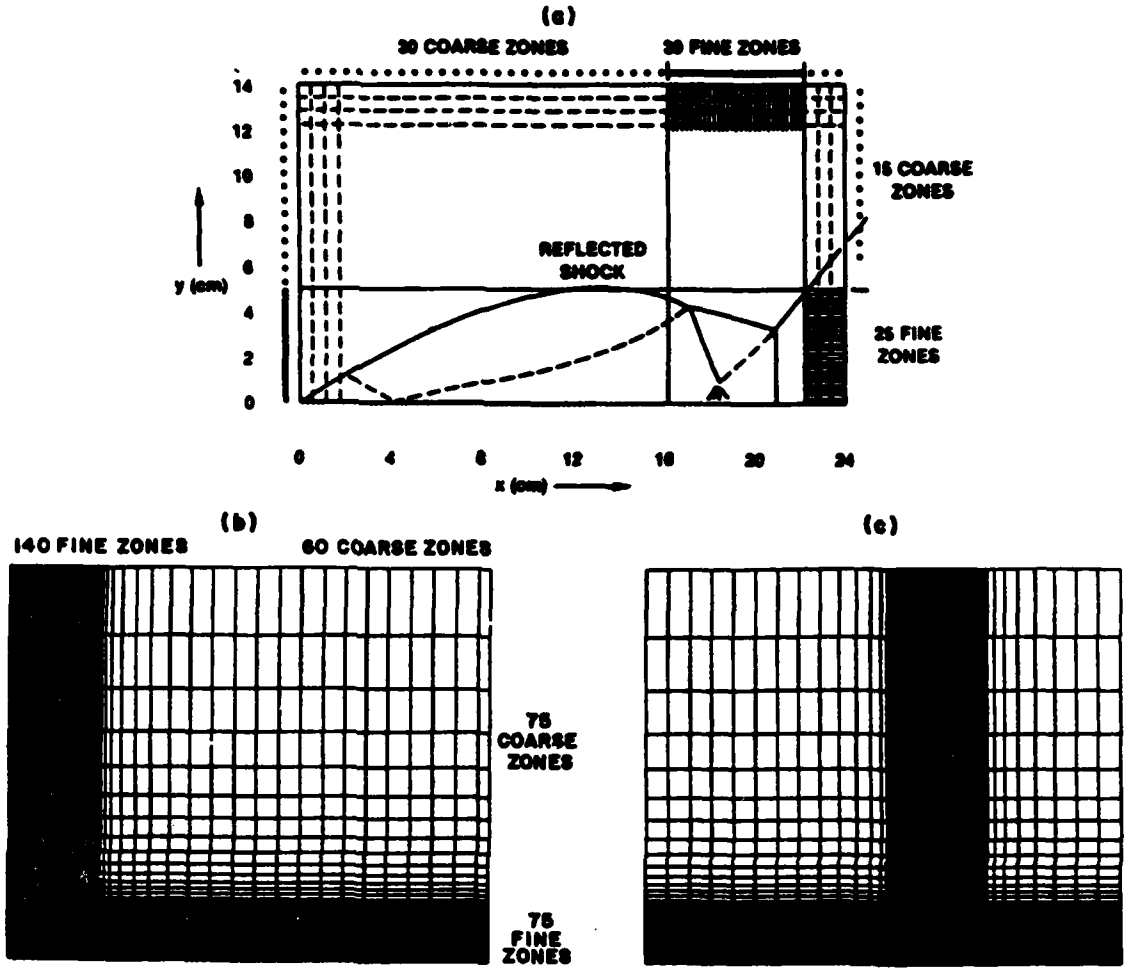

Fig. 1. Adaptive grids for a) planar shocks on wedge (double Mach shock features are indicated); b) and c) HOB problem initially and at transition point (grid lines in fine-zone region are indistinguishable).

SHOCK-ON-WEDGE CALCULATIONS

The JPBFCT algorithm was used in a 2-D Cartesian version of the FAST2D code to model the reflections of planar shocks from wedges of 20° to 60° and varying shock strengths. Four general classes which include regular, single, complex and double Mach reflection were calculated (referred to as cases a,b,c,d respectively). The bottom of the mesh, treated as a reflecting boundary, modeled the surface of the wedge. Quantities on the right hand boundary and on the top were set equal to the ambient values. The remaining boundaries were treated as permeable. In the single, complex, and double Mach reflection cases, the mesh was anchored on the left, essentially at the wedge tip where the incident shock first strikes, while the zones were stretched by a scaling factor proportional to t as soon as the reflection region filled a substantial portion of the grid. In case (d), the double Mach reflection case, the opening angle is so small that the incident shock has to traverse many zones before the mach stem has grown large enough to be well resolved. For this reason, the problem was solved on a uniform mesh in the frame of reference fixed

to the reflection point, with stretching being initiated after the first Mach stem reached ∿ 20 cells in length. The timestep was recalculated at every cycle with a Courant number of 0.5.

Figure 2 shows the pressure and density contours and the velocity field for cases a,b,c,d. The pertinent shock phenomena can be easily identified: incident shock, contact surface, first and second Mach stems. As shown in Fig. 1, the zoning is particularly sparse except for the region of interest. Adequate resolution of the key surfaces (contact and second Mach stem) is obtained with 5 zones in each direction. The accuracy can be evaluated by comparing the experimental density distributions along the wall (Fig. 3).

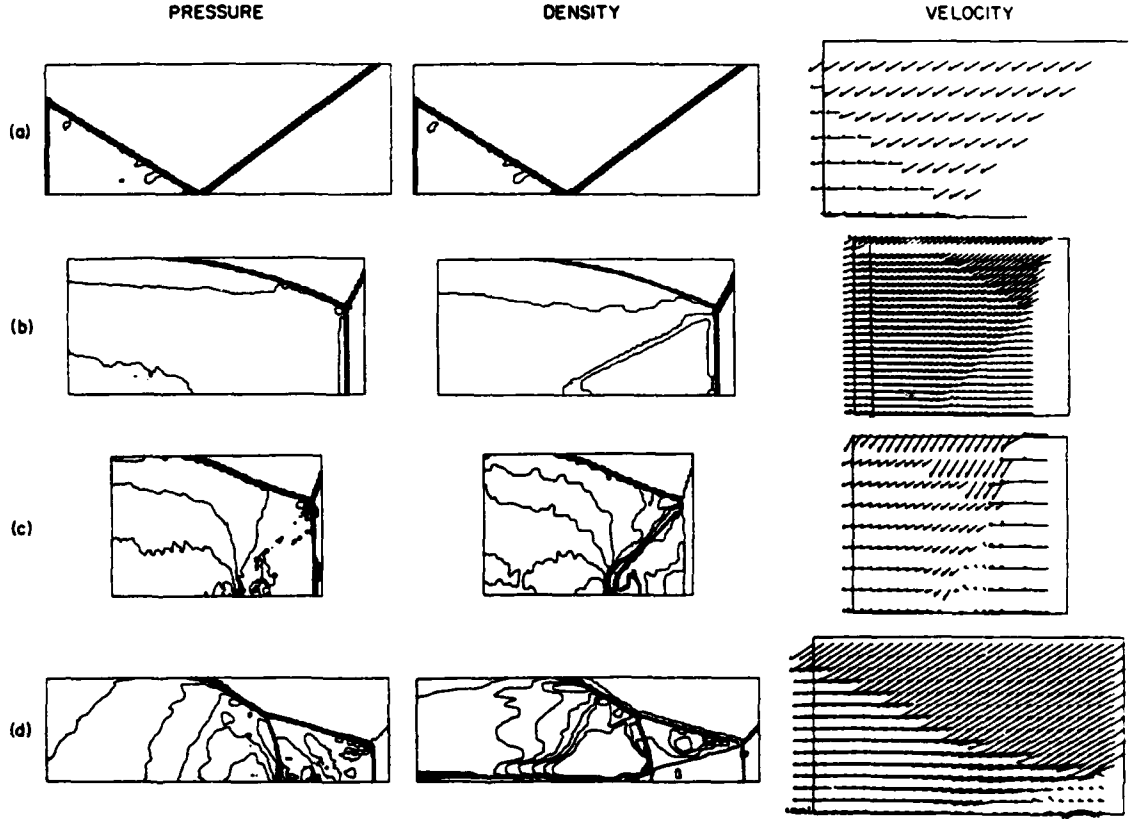

Fig. 2 - Pressure and density contours and flow velocity vectors (in frame of reflection point) for planar waves with Mach number M reflecting from wedges with angle θ for (a) M=2.03, θ=60°; (b) M=2.82, θ=20°; (c) M=5.29; θ=30°; (d) M=7.03; θ=50°

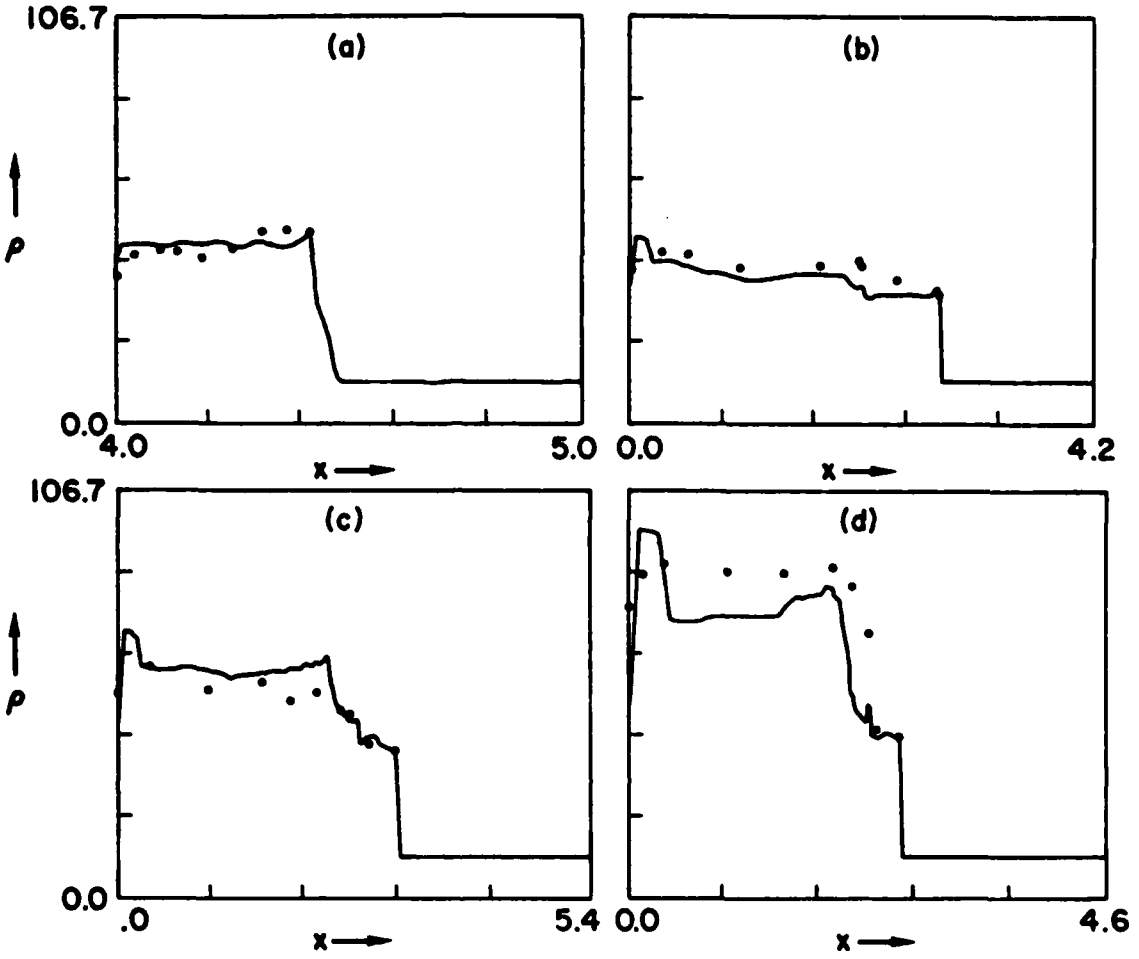

Fig. 3. Comparison of density (in units of ambient density ρ_o) for cases (a), (b), (c), (d) of Fig. 2 vs. distance from corner. Points are measured values reported in Ref. 13.

HEIGHT OF BURST CALCULATIONS

Next, we performed a numerical simulation of a 1KT nuclear detonation at 31.7 m HOB, a case which could be readily compared with high explosive data. A constant ambient atmosphere was used with a density of 1.22×10^{-3} g/cm^3 and pressure 1.01×10^6 dynes/cm^2. To relate the energy and density to the pressure, a real-air equation of state (EOS) was used. This table-lookup EOS was derived from theoretical calculations by Gilmore[14,15] for equilibrium properties of air and has been vectorized for the Advanced Scientific Computer[16]. The internal energy density used in the call to the EOS is found by subtracting kinetic from total energy; this can be negative due to truncation (phase) errors. When this occurred, the value of the pressure was reset to zero.

The transition from regular reflection to double Mach reflection occurs at a ground range approximately equal to the HOB. The size of the mesh should

therefore be roughly twice the HOB in both directions. The upper boundary should be far enough away from the blast front to be non-interfering. We chose boundaries of 55 m for the radial direction and 103.5 m for the axial direction. The fine grid in the radial direction contained 140 out of 200 total zones, each 5 cm in length. The rightmost zones were 80 cm in length, and a smoothing involving 40 zones was performed between the regions to guarantee that the zone sizes varied slowly. In the axial direction the fine grid contained 75 out of 150 total zones, each 5 cm in length. Beyond that region the zones were geometrically increased by a factor of 1.112.

Placement of the fine grid at the origin of the mesh (ground zero, the point at which reflection first occurs) was determined to be optimum for capturing peak pressure in the airblast wavefront. Thus, as the expanding wave moves along the ground surface, the fine grid is always locked to it and each point along the blast front encounters the same spatial gridding as it approaches the ground. By treating each point of the incident front in the same manner, we insure that the calculation is internally consistent and that the computed transition point is accurate to within the limits of the resolution.

The initialization provides a strong shock with approximate Mach number M=12. This speed and the need for restart capability led to the choice of 200 timesteps as an interval for the spatial display (snapshots). The dump interval that resulted was $\Delta t \sim 0.3$ milliseconds (ms). These dumps were stored on magnetic tape and post-processed.

A fit to the 1-D nuclear blast flow field (Ref. 17) was used to initialize the energy and mass density and velocity field at 3.76 ms. The corresponding peak overpressure was 113 bars. After the 1 KT flow field was laid down inside a radius of 31.6 m, the fine-zone grid was activated to follow the peak pressure as it moved along the ground surface, modelled as a perfectly reflecting boundary. This region comprised 140 zones, and a switch was set to keep 40 of these zones ahead of the reflection point. Permeable boundary conditions are used on the top and right edges of the mesh, i.e., density, pressure and velocity are set equal to ambient preshock conditions. Reflecting conditions were applied to the left and bottom. The total elapsed physical time in the 2-D calculation, 7.6 ms, required 5600 cycles. Times are referred to t=0 at the start of the calculation.

The numerical simulation begins just before the shock first reflects from the ground. Fig. 4a indicates the pressure and density contours and velocity vectors at time 3.18 ms. In Fig. 4b the reflected shock is shown moving upward, the outward flow begins to stagnate at the ground (transition). Fig. 4c, t=5.99 ms, shows an enlargement of the shockfront, and the development of the Mach stem, slip surface and second Mach stem. The angle of the shock front with respect to the ground is increasing with time, so that the effective wedge angle is decreasing. From Ben-Dor and Glass[18] one expects a transition to double Mach stem to occur at approximately 45°. The angle in Fig. 4b is about 45° and the shock front has entered the transition phase. Figure 4d shows the fully developed shock structure at 7.79 ms. Clearly visible is the second Mach stem and a vortex region behind the first Mach stem. Toeing out of the first Mach stem can be also seen in the contours of Fig. 4d and occurs as the fluid rolls forward where the slip line would otherwise intersect the ground. The velocity field in Fig. 4d also shows this detail.

One should also note the reflected shock properties. The reflected shock propagates rapidly through the high temperature fireball, due to the high local soundspeed. The shape of this reflected wave is a primary difference between the HOB case and the wedge case[19]. The other major difference, of course, is the spherically expanding blast wave which decreases in strength approximately proportional to r^{-2}.

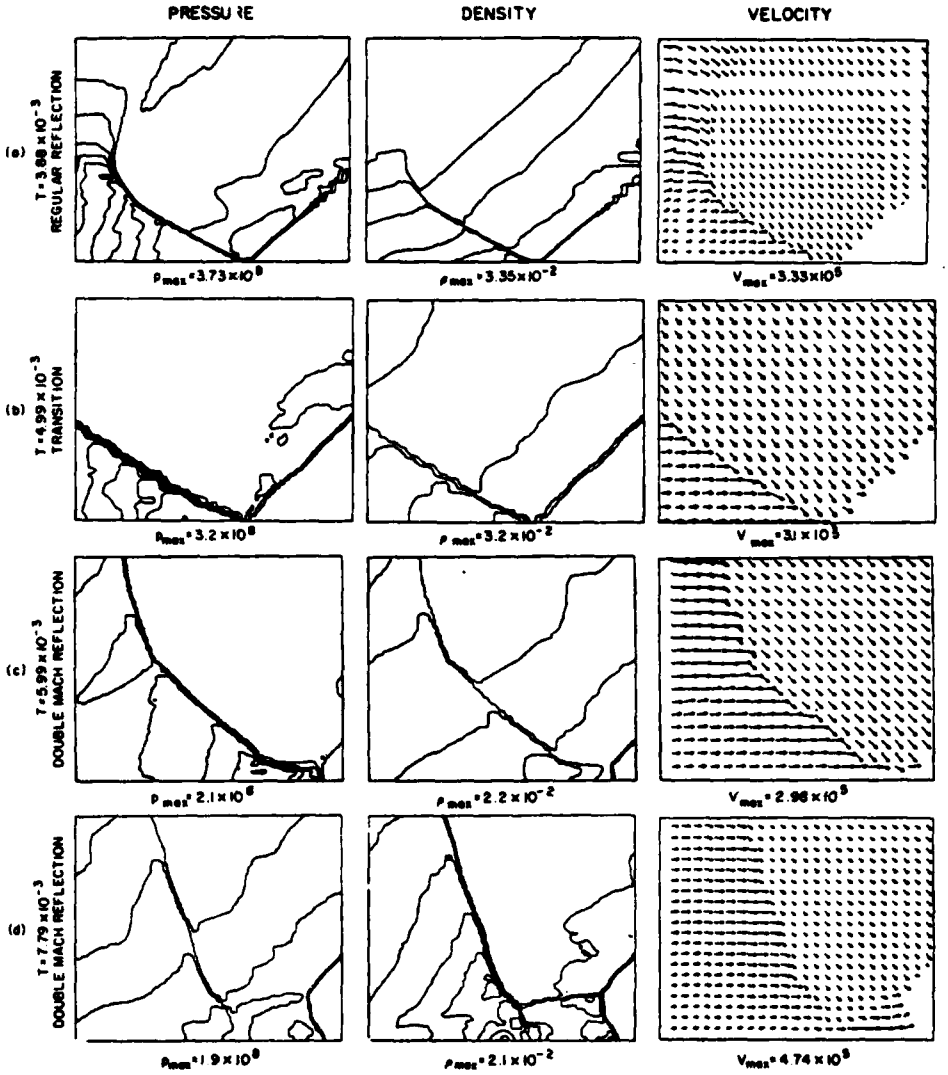

Fig. 4. Pressure, density, and velocity fields for HOB calculation (a) in regular reflection stage; (b) at transition to Mach reflection; (c) shortly afterward, when second peak has become larger than first; and (d) fully developed (note toe at base of first Mach stem).

Finally we consider the pressure/distance relation for the HOB case. In Fig. 5 we compare the results of the numerical simulation with the data of Carpenter and with empirical analysis. Carpenter's data are based upon careful HOB experiments with 8 lb PBX9404 spheres. The empirical analysis was based on a 1 KT nuclear free air curve and HOB construction factors. The calculated values in the regular reflection regime are 20% low and may be attributed to a combination of FCT clipping, the resolution of the grid, and inaccuracies in the initialization of the flow field. During and after Mach reflection, the peaks remain low until the Mach stem structure has grown large enough to be resolved on the mesh. By the time it occupies a region of 15 cells high and 35 cells wide, the peak pressures are in good agreement with the HE data and the empirical analysis.

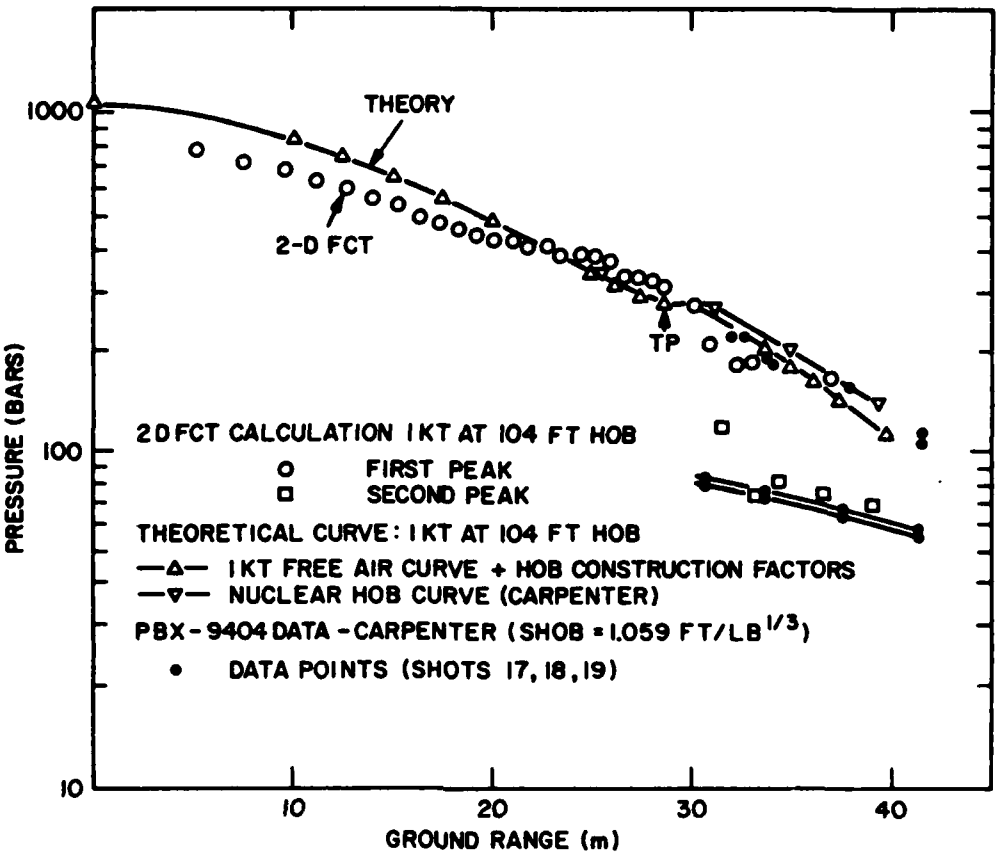

Fig. 5. Pressure-range curves for first and second (after transition - denoted by TP - to double Mach reflection) peaks.

SUMMARY AND CONCLUSION

The complex 2-D Mach reflection phenomena associated with shock diffraction on wedges and height-of-burst explosions have been modeled with the FAST2D computer code. Four wedge cases--regular, single, complex and double Mach reflection—have been calculated and the results compared to experiments. A nuclear detonation (1 KT at 31.7m HOB) was also simulated. The results give insight into the formation and subsequent evolution of the Mach stem, the triple point and the contact discontinuity. The transition from regular reflection to double Mach reflection is predicted. Excellent agreement with Ben-Dor's data is obtained. We suggest that the first signal for transition is the appearance of a second peak behind the shock front due to stagnation in the flow. Calculated first and second pressure peaks versus distance in the HOB case agree both with the HE data and analysis to within 20%.

The use of the adaptive regridding procedure, called "sliding rezone", along with the FCT algorithm allows one to accurately predict the nonsteady shock structures in two dimensions for diffractions on wedges and HOB cases. Comparison with data for both wedges and HOB yields the best results obtained to date.

ACKNOWLEDGEMENT

This work was supported by the Defense Nuclear Agency under Subtask Y99QAXSG, Work Unit 00001, and Work Unit Title "Flux-Corrected Transport."

REFERENCES

1. Von Neumann, J., "Oblique Reflection of Shocks", Explosive Research Report No. 12, Navy Department, Bureau of Ordinance, Re2c, Washington, D.C. (1943).
2. Taub, A. H., "Refraction of Plane Shock Waves", Rev. Mod. Phys., Vol. 21, p. 51 (1947).
3. Bleakney, W., and Taub, A. H., "Interaction of Shock Waves", Rev. Mod. Phys., Vol. 21, p. 584 (1949).
4. Lighthill, M. J., "On the Diffraction of Blast I", Proc. Roy. Soc., Vol. 198, p. 454 (1949), Vol. 200, p. 554 (1950).
5. Jones, D. M., Martin, P. M., and Thornhill, C. K., "A Note on the Pseudo-Stationary Flow Behind a Strong Shock Diffracted or Reflected at a Corner", Proc. Roy. Soc., Sec. A, Vol. 209, p. 238 (1951).
6. Shankar, V., Kutler, P., and Anderson, D., "Diffraction of a Shock Wave by a Compression Corner - Part II, Single Mach Reflection", AIAA Journal, Vol. 16, No. 1 (1977).
7. Ben-Dor, G., and Glass, I., "Nonstationary Oblique Shock Wave Diffractions in Nitrogen and Argon - Experimental Results", UTIAS Tech Note (1978).
8. Courant, R., and Friedrichs, K. O., "Supersonic Flow and Shock Waves", Interscience Publishers, New York (1948).
9. Booen, M., and Needham, C., "Two-Dimensional Hull Code Simulation of Complex and Double Mach Reflections", AFWL NTE TN 81-001 (1981).
10. Boris, J., and Book, D., "Flux-Corrected Transport: I SHASTA, A Fluid Transport Algorithm that Works", J. Comp. Phys., 11, 38 (1973).
11. Oran, E. S., Young, T. R., Jr., and Boris, J. P., "Applications of Time-Dependent Numerical Methods to the Description of Reactive Shock", Proc. 17th Symposium (International) on Combustion, The Combustion Institute, Pittsburgh (1979).
12. Boris, J. P., "Numerical Solution of Continuity Equations", NRL Memo Report 3327 (1976).
13. Ben-Dor G,and Glass, I.,"Domains and Boundaries of Non-Stationary Oblique Shock-Wave Reflections, II Monatomic Gas", J. Fluid Mech., 96, p. 735 (1980).
14. Gilmore, F. R.,"Equilibrium Composition and Thermodynamic Properties of Air to 24,000°K" RAND Corp, RM-1543 (24 August 1955).
15. Gilmore, F. R., "Equilibrium Thermodynamic Properties of High Temperature Air", Lockheed Missile and Space Co., DASA 1917-1 (April 1967).
16. Young, T. R., (Private Communication 1981).
17. Needham, C., et. al., Nuclear Blast Standard, AFWL 7R-73-55, Air Force Weapons Laboratory (April 1975).
18. Ben-Dor, G., Glass, I., "Domains and Boundaries of Non-Stationary Oblique Shock-Wave Reflections Diatomic Gas", J. Fluid Mech., Vol. 92, part 3, p. 459 (1979).
19. Book, D., et. al., "Two-Dimensional FCT Model of Low Altitude Nuclear Effects", NRL Memo Report 4362 (1980).
20. Carpenter, H. J., "Height of Burst at High Overpressures", 4th International Symposium on Military Applications of Blast Simulation (1974).

Appendix B

A THEORETICAL STUDY OF THE IGNITION OF PRE-MIXED GASES

by:

K. Kailasanath
Science Applications, Inc.
McLean, Virginia 22102

and

E. Oran and J. Boris
Laboratory for Computational Physics
Naval Research Laboratory
Washington, D.C. 20375

ABSTRACT

In this paper, time-dependent results obtained from both a simple but nonlinear analytic similarity solution and a detailed numerical simulation model are used to study the interactions between the fundamental processes occurring in the ignition of homogeneous premixed gases. The parameters which may be varied are the composition of the mixture, the initial radius of energy deposition R_o, the duration of the heating τ_o, and the total energy deposited in the system E_o. The similarity solution plus the induction time for the fuel-oxidizer mixture as a function of temperature and pressure can be used to calculate whether or not a given energy source is adequate to ignite the system. This simple procedure is then calibrated using a time-dependent detailed numerical reactive flow model which includes the thermophysical properties of the mixture, a full chemical kinetics scheme, nonlinear convection, molecular diffusion and thermal conduction. Calculations are presented for a selected mixture of H_2-O_2-N_2 for various values of R_o and E_o. These show that the similarity solution predicts ignition accurately when the radius of energy deposition is larger than the quench-radius. The detailed numerical reactive flow model is used to predict the quench-radius and the absolute minimum ignition energy associated with it.

NOMENCLATURE

A	Nonlinear amplitude in similarity solution
E	Energy
E_o	Total amount of energy deposited
I	Induction Parameter
k	Scale size in similarity solution
k_B	Boltzmann's constant
N	Total number density
n_j	Number density of species j
P	Pressure
P_j	Term representing production of species j
Q_D	Contribution to the heat flux vector due to diffusion
Q_j	Term representing loss of species j
R_o	Initial radius of deposition
R_c	Characteristic radius of energy deposition
r	Radial distance
T	Temperature
t	time
v	fluid velocity
V_j	Diffusion velocity of species j
γ	ratio of specific heats, c_p/c_v
η_m	mixture viscosity coefficient
λ_m	mixture thermal conductivity coefficient
ρ	mass density
τ_o	time period during which energy is deposited
τ_c	chemical-induction time

INTRODUCTION

An external source of energy can initiate interactions among the controlling convective, diffusive and chemical processes in a fuel-oxidizer mixture. Whether the interactions result in ignition of a deflagration or detonation wave depends on the intensity, duration, and volume affected by the external heat source. Ignition will also depend on the initial ambient properties of the mixture which determine the chemical induction time and the heat release per gram of material. Thus ignition is a complicated phenomena whose occurrence for a specific mixture of fuel and oxidizer depends strongly on diffusive and chemical parameters which are often very poorly known.

It is possible, in principle, to study flame ignition by performing detailed numerical simulations. This is a complicated, multi-dimensional, multi-species, time-dependent problem which has been solved in certain limited cases (see e.g., Ref. 1). Part of the complication and cost of such calculations arises from the multi-dimensional solution of the conservation equations, but at least as much arises from integrating the large number of ordinary differential equations describing the chemical reactions. This latter factor is further complicated by the fact that we usually do not have an adequate representation of the chemical reactions with which to work. Thus a convenient, inexpensive way to estimate whether a mixture will ignite given a heat source intensity, duration, and volume would be a very valuable laboratory tool and a useful learning device.

This paper represents an extension and clarification of the work described by Oran and Boris [1,2]. They presented a preliminary summary of a simplified, theoretical model of localized ignition of a homogeneous, premixed gas and explained how it could be calibrated by using a detailed simulation. In this paper the calibration of the simplified model is extended and the results are compared in detail to those of detailed, one-dimensional simulations. After a brief review of related literature, the essential properties of the detailed, time-dependent, numerical model are presented. Then a description is given of a closed form similarity solution for the nonlinear time-dependent slow flow equation which forms the basis for the simplified model of localized ignition. The similarity model avoids the integration of the ordinary differential equations describing the chemical reactions by defining an induction parameter. Two constants must be calibrated; the radius at which the thermal conductivity is evaluated and the radius at which the induction parameter is evaluated. Finally, comparisons between the two models are described for ignition of a H_2-O_2-N_2 mixture. The composition of the mixture and the duration of energy deposition are held constant but the total energy deposited and the radius of deposition are allowed to vary.

BACKGROUND

Ignition phenomena and the associated properties of minimum ignition energies and quench volumes have been studied both experimentally and theoretically. Lewis and von Elbe [3] have reported extensive experimental data on ignition by electric sparks. Weinberg and Wilson [4] and Kingdon and Weinberg [5] have compared the ignition energies required when a spark and a laser were the source of ignition. The former paper [4] concludes that the laser minimum ignition energy is very much less than that required by a spark for mixtures at low pressures or near the flammability limit. They have attributed this difference to the influence of the electrodes and the losses to them since the quenching distances are large under the above conditions. The latter paper [5] concludes that for short pulses applied to mixtures with small quenching distances, the energies required by the two ignition sources are not that different.

Dixon-Lewis and Shepherd [6] have used a time-dependent flame model to examine the effects of varying the initial radical concentration and of changing the geometry of the initial hot core. Their studies were done on a homogeneous premixed 60% hydrogen-air mixture in which energy was deposited instantaneously in the form of hydrogen atom radicals and temperature. They found that energy in the form of hydrogen atoms was more efficient at igniting a flame. Dixon-Lewis [7] then looked for a minimum quench volume in the same 60% hydrogen-air mixture in which one third of the added energy was in the form of hydrogen atoms.

Another point noted by both Overley et al. [8] and by Dixon-Lewis and Shepherd [6] is that the shape and size of the mixture core is important in determining the minimum ignition energy. The former paper presented a study of a hydrazine mixture in both spherical and prolate spheroidal coordinates. The latter paper considered both cylindrical and spherical systems. Both papers investigated the effects of flame curvature on burning velocity.

The work of Ballal and Lefebvre [9] is a detailed experimental investigation of the effects of pressure, velocity, turbulent intensity and scale, and mixture composition on the minimum ignition energy and quench distance in a flowing gas mixture. Using the data as a guide, they analyzed the important transport and turbulent processes and developed a highly simplified model for the quench distance in the limit of low and high turbulence. The data has allowed them to calibrate the model and determine important constants.

THE DETAILED NUMERICAL SIMULATION MODEL

This section describes the detailed numerical flame model which solves the time-dependent conservation equations for total mass ρ, momentum ρv, energy E, and individual species densities n_j [2,10]:

$$\frac{\partial \rho}{\partial t} = -\underline{\nabla} \cdot \rho \underline{v} \tag{1}$$

$$\frac{\partial n_j}{\partial t} = -\underline{\nabla} \cdot n_j \underline{V}_j - \underline{\nabla} \cdot n_j \underline{v} + P_j - Q_j n_j \tag{2}$$

$$\frac{\partial \rho \underline{v}}{\partial t} = -\underline{\nabla} \cdot (\rho \underline{v}\underline{v}) - \nabla P + \underline{\nabla} \cdot \eta_m [\underline{\nabla v} + (\underline{\nabla v})^T] \tag{3}$$

$$\frac{\partial E}{\partial t} = -\underline{\nabla} \cdot E\underline{v} - \underline{\nabla} \cdot (P\underline{v} - \lambda_m \underline{\nabla} T - \underline{Q}_D) \quad . \tag{4}$$

The technique for solving the various terms in these equations is based on the method of asymptotic timestep splitting in which the individual chemical and physical processes are integrated separately and then asymptotically coupled together [1]. The model permits a wide variety of geometric, initial, boundary and time-varying energy input conditions and was specifically developed to study the various physical and chemical processes which control flame initiation and quenching [23].

The convective transport is solved by the algorithm ADINC, a Lagrangian hydrodynamic algorithm which solves implicitly for the pressures [11]. The method allows for arbitrary equations of state, gives an accurate representation of material interfaces, and allows steep gradients in species and temperature to be developed and maintained.

A number of tests of this algorithm have been documented by Boris [11] . An adaptive gridding method has been implemented in which cells are inserted or deleted according to externally specified physical conditions in the flow. The diffusion velocities are calculated using an iterative algorithm [12,1].

The chemical interactions are described by a set of nonlinear coupled ordinary differential equations. For this ignition study we have used the H_2-O_2 reaction scheme [13] given in Table 1 which involves the eight reactive species, H_2, O_2, O, H, OH, HO_2, H_2O_2, H_2O and diluent which is chosen to be N_2. The thermochemical properties of these species were taken from the JANAF tables [14]. The ordinary differential equations describing the chemical kinetics are solved using a fully vectorized version of the selected asymptotic integration method, CHEMEQ, developed by Young [15,16].

Results from a typical flame calculation in spherical geometry are presented in Fig. 1. The figure depicts the time history of the temperature profile after 4mJ of energy is deposited over a period of 10^{-4} seconds. Even after the energy deposition is stopped the "core" temperature continues to increase due to the heat released in chemical reactions. With time, however, the temperature near the center decreases and the temperature away from the center increases due to heat conduction. In this case, since the rate of heat generation is greater than the rate of heat loss, the temperature profile develops into that of a typical flame temperature profile. Species profiles and details of the flame front have been presented elsewhere [2].

THE SIMILARITY SOLUTION

The similarity solution is derived from the slow flow approximation [1,17] and is predicated on the assumption that energy addition to the system is slow enough so that there is no shock heating. Thus the system is characterized by flow velocities which are small compared to the speed of sound, and an essentially constant pressure field. The energy and velocity equations may be written in terms of total derivatives as

$$\frac{dP}{dt} \approx 0 = -\gamma P \underline{\nabla} \cdot \underline{v} + \underline{\nabla} \cdot \gamma N k_B \kappa \nabla T + S(t) e^{-k^2(t) r^2} \qquad (5)$$

and the continuity equation is written in the form

$$\frac{1}{\rho} \frac{d\rho}{dt} = -\underline{\nabla} \cdot \underline{v}. \qquad (6)$$

In Eq. (5) γ is held constant, and κ is a function of the mixture thermal conductivity, λ_m,

$$\kappa \equiv \frac{\gamma - 1}{\gamma N k_B} \lambda_m(T) \ . \qquad (7)$$

The last term on the right hand side of Eq. (5) is the source term. Proper choice of S(t) ensures that a given amount of energy, E_o, is deposited in a certain time, τ_o. It is the choice of this Gaussian profile which allows us to obtain the "closed" form similarity solution which is given below.

The details of the solution of Eqs. (5) and (6) are given in the Appendix at the end of this paper. The final results for the temperature and density as a function of time and position may be written as

$$T(r,t) = T_\infty e^{A(t)e^{-k^2(t)r^2}} \tag{8}$$

and

$$\rho(r,t) = \rho_\infty e^{-A(t)e^{-k^2(t)r^2}} \tag{9}$$

where T_∞ and ρ_∞ are the background temperature and density, respectively. In addition, two ordinary differential equations describing the evolution of A(t) and k(t) are required to complete the solution,

$$\frac{dk}{dt} = - kv_1 - 2Kk^3 \tag{10}$$

$$\frac{dA}{dt} = \frac{S(t)}{\gamma P_\infty} - 2ck^2 A \tag{11}$$

where v_1 is an approximation to the velocity based on the assumption that $v(r,t) \equiv v_1(t)r$; and c is a constant which depends upon the configuration of the problem (c = 1 for cartesian, 2 for cylindrical and 3 for spherical coordinates). By comparing the results from this similarity solution model to those from the detailed numerical simulation model described earlier, we have seen that the linear dependence on r is a valid approximation before ignition occurs.

The model requries one further defintion in order to predict ignition. The chemical induction time, which is a function of temperature and pressure, must be used to define the induction parameter,

$$I(T,P) = \int_0^t \frac{dt'}{\tau_c\left[T(r,t'),\ P(r,t')\right]} \ . \tag{12}$$

For the work presented in this paper, pressure is constant throughout the calculation. Then $I(T,P_\infty)$ is integrated in time according to Eq. (12). Ignition "occurs" when $I(T,P_\infty) = 1$, which is an exact result in the limit of large heat source and constant temperature near the center of the heated region. Values of τ_c have been calculated [13] for a wide range of temperatures and pressures from the chemical rate scheme given in Table I. In general, τ_c as required in these calculations may be obtained from such detailed kinetic calculations, a few measured points, or from educated guesses. The concept of an induction parameter has been extended in scope and used extensively for reactive shock and detonation studies [e.g., 1, 18, 22].

The parameter κ in Eqs. (10) and (11) is found using the definition in Eq. (7). Determining the temperature (radius) at which κ is to be evaluated is part of the calibration to be done. For this, the derivation in the appendix was also done for the case where κ was assumed to be a function of radius (r). This analysis indicated that if k is to maintain its similarity form and be a function of time alone, κ must be independent of r. Thus, within the framework of the similarity solution, the appropriate location at which to evaluate κ is at the center ($r = 0$). Determining the location at which the induction parameter, $I(T,P_\infty)$, should be evaluated is the second calibration to be done. This has been done by comparing the predictions of the two models and is discussed in the next section.

In summary, the approximations to Eqs. (1) - (4) which allows us to write Eq. (5) and obtain the solutions represented by Eqs. (8) - (11) are:

1. The flow velocities characteristic of the system are small compared to the speed of sound;
2. The pressure is essentially constant everywhere;
3. The ratio of specific heats, γ, is constant;
4. Molecular diffusion effects are not important until after ignition;
5. The velocity, $V(r,t)$ may be approximated by $V_1(t)r$;
6. The system is homogeneous and premixed;
7. The energy is input in a Gaussian form with a characeristic radius R_c which increases in time; and
8. The gas never gets hot enough to radiate away a significant fraction of its energy during the ignition period.

MODEL COMPARISONS

The calibration of the similarity model is complete when the location at which the induction parameter should be evaluated is determined. For this purpose, the results from detailed simulations are compared to those from the similarity model. Energy deposition in both models is linear in time at a rate determined by requiring an energy E_o to be deposited in a time τ_o. For all of the results discussed in this paper, τ_o is taken to be 10^{-4} seconds. As in the similarity model, energy deposition in the detailed model is in the form of a Gaussian profile in space. The characteristic radius of the Gaussian, R_c, increases with time and is determined in the detailed simulation by the formula:

$$R_c^2 = \frac{2\int r^2 \ell n\,(T/T_\infty)\,dr}{\int \ell n\,(T/T_\infty)\,dr} \tag{13}$$

The chemical model for these first tests was taken to be a mixture of $H_2:O_2:N_2$ in the ratio 2:1:10 at 1 atm and $T_\infty = 300^oK$. The induction time as a function of temperature for this mixture was derived from the detailed studies of the H_2-O_2 reaction mechanisms [13] and is shown in Fig. 2.

In the similarity model, κ was estimated by comparing the formula at 300^oK,

$$\lambda_M^S = \frac{8.4 \times 10^3}{\bar{\sigma}^2}\sqrt{\frac{T(^oK)}{\bar{M}}}\ \frac{erg}{cm\ sec\ ^oK}, \tag{14}$$

which assumes that an average molecular distance $\bar{\sigma}$ and an average molecular weight $\bar{M}$ may be found, to the more exact formulation

$$\lambda_m = \sum_j \lambda_j \left[1 + \frac{1}{2\sqrt{2}} \sum_{k\neq j} n_k W_{jk}\right]^{-1} \tag{15}$$

where W_{jk} is a function of $\{\lambda_j\}$ and the atomic masses $\{m_j\}$ suggested by Mason and Saxena [19]. This gives us

$$\bar{\sigma} = 3.16\ A$$
$$\bar{M} = 24.3. \qquad (16)$$

This approximation is valid because the similarity solution is only accurate for ignition, that is, before any major amount of product or intermediates are formed. Then the parameter κ is found using the definition in Eq. (7). As discussed in the previous section, for the similarity solution κ is evaluated at the central (r=0) temperature. In contrast the detailed simulation uses Eq. (15) to evaluate the thermal conductivity at each cell at each time step.

In the first case studied, the initial radius of deposition, R_o, was 0.1 cm and both models were configured for spherical symmetry. By varying E_o and evaluating the induction parameter $I(T,P_\infty)$ at the central temperature (r=0) the similarity solution indicates that the minimum ignition energy is about 3.7mJ. Figure 3 shows the typical behavior of the amplitude, A(t), and the characteristic radius, R_c, for this test case. If $I(T,P_\infty)$ is evaluated at R = 0.06 cm the minimum ignition energy predicted is about 5.1mJ, and if it is evaluated at R_c ignition is not predicted even when E_o is raised to 8mJ. By comparing these predictions with those from the detailed simulation model we determine the location at which $I(T,P_\infty)$ must be evaluated. Results from the detailed simulation are shown in Fig. 4 for three values of E_o. Ignition occurs when E_o is greater than or equal to 3.7mJ. Therefore good agreement between the two models for the case under study is achieved by evaluating the induction parameter at the central temperature.

The central temperature and the induction parameter have been shown for three values of E_o in Figs. 5 and 6 respectively. The time at which ignition occurs (I = 1.0) is shown by a '*' in Fig. 6. A comparison with the

results from the detailed simulation (Fig. 4) tells us that both models predict ignition at essentially the same time for a range of input energies. The temperature profiles predicted by the two models are presented in Fig. 7. The agreement is very good except for long times when the detailed simulation predicts higher temperatures than those from the similarity model. This is primarily due to the heat released in chemical reactions which is not included in the similarity model. It is interesting to note that the effects of molecular diffusion included in the detailed simulation model are not considered in the similarity solution model. The results presented have shown that these effects are not as important as the effects of thermal conduction in determining the ignition characteristics of the system under investigation.

The models were then re-configured for cylindrical geometry and the case, R_o=0.1cm, was again investigated. By varying E_o, the similarity solution indicates that the minimum ignition energy is about 3.5mJ/cm, not very different from the spherical case. The detailed simulation predicts that the minimum ignition energy is between 3.3 and 3.7mJ/cm, so again the predictions of both models are comparable when the induction parameter is evaluated at r=0.

EFFECT OF QUENCHING DISTANCE

As discussed in the previous section, good agreement between the predictions of the detailed simulation and the similarity solution is obtained for the case, R_o = 0.1 cm. In order to determine if the agreement is good for other values of R_o, various cases were studied and these have been summarized in Table II. Evaluating the induction parameter at the central temperature provides agreement between the ignition predictions of the two models for all the cases in which R_o is greater than 0.1 cm. However, for radii smaller than 0.1 cm the similarity solution predicts a minimum ignition energy that is lower than for the R_o = 0.1 case described above. In fact, as the initial radius of deposition decreases below 0.1 cm the similarity solution (with $I(T,P_\infty)$ evaluated at a fixed radius) predicts that the minimum ignition energy also decreases. The detailed simulation does not agree with this prediction. The radius 0.1 cm appears to be a "critical radius" below which the minimum ignition energy again increases. The above observation is similar to that made by Blanc, Guest, von Elbe and Lewis [20]. In their study of spark ignition, it was observed that there was a "critical electrode spacing" below which the minimum ignition energy increased. The critical electrode spacing was termed the "quenching distance".

To study the phenomena of "absolute" minimum ignition energies and quenching distances, the energy deposition in the detailed simulation needs to be modified. Up to this point energy was deposited in a Gaussian profile with a characteristic radius which increased with time. This was necessary in order to ensure that energy was deposited in a manner which closely matches the one derived from the similarity model. In the similarity model,

a Gaussian profile with characteristic radius increasing in time was essential to obtain the similarity solution described earlier. However, for studying the effect of the radius of deposition on the minimum ignition energy, it is confusing to have a varying radius of deposition. Therefore, for the results discussed below, energy is deposited in a Gaussian profile with a constant radius of deposition. As before, energy deposition is linear in time at a rate determined by requiring an energy E_o to be deposited in a time τ_o.

For a particular radius of deposition, a certain amount of energy is deposited and the computations are carried out for sufficient time until the existence (or absence) of a propagating flame is definite. By repeating the computations for different values of E_o a bound for the minimum ignition energy for that particular radius is obtained. Similar calculations are performed for different values of the radius of deposition, R_o. The results of such investigations are shown in Fig. 8. A propagating flame results when 3.8 mJ of energy is deposited in a sphere with a radius of 0.1 cm. However if the same amount of energy is deposited in a sphere of smaller radius, the rate of heat liberation is insufficient to compensate for the rate of heat loss and consequently there is no ignition. This radius, 0.1 cm, is the "quench-radius" for this particular mixture. For radii slightly larger than the quench-radius, the minimum ignition energy is almost constant and for larger radii (larger than 0.11 cm) the minimum ignition energy increases rapidly with increasing radii. Therefore for the system under study, the

absolute minimum ignition energy is about 3.7 mJ. These observations are in qualitative agreement with those of Lewis and von Elbe [21]. Quantitative comparisons are not possible since the composition of the mixture and the time for energy deposition are different.

This study of the "quench-radius" provides the insight needed to explain the discrepancy in the predictions of the similarity solution and the detailed model for small radii. We conclude that a volume smaller than the "quench-volume" needs to be maintained at a temperature T for a time which is longer than the corresponding induction time for ignition to occur. Therefore the concept of an induction parameter as it is used in the similarity solution is not valid for very small radii. If the absolute minimum ignition energy is deposited in a sphere of radius smaller than the quench radius, ignition will not occur since the heat generation rate within this smaller volume cannot compensate for the heat loss rate. This effect is not significant in measurements of induction time which are for larger radii. Therefore an agreement between the predictions of the two models can be forced for radii smaller than the quench-radius by evaluating the induction parameter at increasingly larger radii (i.e. lower temperatures). For example, when the initial radius of deposition is 0.08 cm, the detailed simulation predicts that the minimum ignition energy is between 3.4 and 5 mJ. The minimum ignition energy predicted by the similarity solution is 3.4 mJ if the induction parameter is evaluated at 0.06 cm and it is 5.1 mJ if the induction parameter is evaluated at 0.08 cm. For the case when the quench radius, r_q = 0.1 cm, the formula

$$r = r_q - Ae^{BR_o}; \qquad (17)$$

$A = 2.84 \times 10^{-4}$ and B = 58.78 gives a good estimate for the radius at which to evaluate the induction parameter. We are currently seeking a more general formula to give this radius.

SUMMARY AND CONCLUSIONS

This paper describes a theoretical model for flame ignition based on a similarity solution which may be used to predict the ignition properties of a homogeneous mixture of gases. The model requires specification of the amount of energy input, E_o, the length of time over which the energy is deposited, τ_o, and the radius of energy deposition, R_o. The model also requires basic information about the gas mixture which includes estimates of the thermal conductivity and the chemical induction time of the gas mixture as functions of temperature. Since a number of approximations have been applied to derive the model, it has been calibrated and its range of validity determined. This has been done by comparing its predictions to those of detailed numerical simulations.

The one-dimensional detailed numerical simulation used solves the set of coupled partial differential equations representing conservation of mass, momentum, and energy as well as individual species densities. For this study it was configured with an open boundary at one end to simulate an infinitely large system. Energy was deposited linearly with time, as it was done in the similarity solution, and the radius of deposition was chosen to mimic that determined by the characteristic radius in the similarity solution. The detailed model, however, contained calculations of the thermal conductivity and chemical kinetics which were much more accurate than the approximations used in the similarity solution. Furthermore, the detailed model contained the effects of molecular diffusion, which were not at all included in the similarity solution.

Predictions from the similarity model consist of an answer as to whether or not a given mixture would ignite given E_o, τ_o, and R_o. Then if ignition is predicted, the model gives the time it takes for ignition to occur. In

contrast, the detailed simulation model not only predicts ignition, but also provides the structure of a propagating flame.

Comparisons of the predictions of the two models show that the system center is the optimal location for evaluation of an induction parameter, which is the indicator of ignition in the similarity model. Furthermore, the predictions of the similarity model are excellent when energy is deposited in a large enough volume. When the radius of deposition is less than the quench radius of the system, the similarity model is not accurate: the similarity model predicts ignition when the detailed model shows it does not occur. This can be compensated for by evaluating the induction parameter away from the system center. However, as with the value of the quench radius, the radius at which the induction parameter must be evaluated can be determined by comparisons with experiments or calculations performed with a detailed model.

After performing a series of studies which tested and calibrated the similarity model in cylindrical and spherical geometries, the detailed model was reconfigured to evaluate the quench radius and the minimum ignition energy of a particular gas mixture. This study provided insight into the source of the disagreement between the predictions of the similarity and detailed models at very small radii of energy deposition. The error occurred because the definition of an induction time is only valid for a volume of material that is large and homogeneous enough in temperature and pressure so that diffusive effects are not important. In the cases where the radii of deposition were very small, increased thermal conductivity due to a steep temperature gradient eroded the high temperature region too quickly. Thus in the competition between chemical energy release to heat a region and thermal conduction to cool it, thermal conduction dominated.

Further limits of validity of the simplified model should now be tested. These include investigating the sensitivity of predictions to time or mode of energy deposition, to variations in the chemical induction time, and to the effects of radiative losses discussed in the Appendix. These kinds of calibrations and determinations of the limitations and sensitivity of the similarity model are extremely important if we are to establish the level of accuracy required for input data. Once this has been done, the similarity model can be used with experimental input data to estimate quickly whether a material is flammable and if so, how much energy is required to ignite it. Another extension of the work presented here involves using the detailed simulation to investigate the effect of geometry and method of energy deposition on ignition energies and quenching distances. Both these studies are currently being pursued.

ACKNOWLEDGEMENTS

The authors would like to acknowledge the help and encouragement of Drs. T. R. Young and H. Carhart in preparing this work. This research has been sponsored by the Naval Material Command and the Naval Research Laboratory through the Office of Naval Research.

APPENDIX

The derivation of the similarity solution model is discussed in detail here for the case of spherically symmetric geometry. Assuming that the pressure field is essentially constant and that no shocks are present, the conservation equations for momentum and energy may be combined to give

$$\frac{dP}{dt} \approx 0 = -\gamma P \underline{\nabla} \cdot \underline{v} + \underline{\nabla} \cdot \lambda N k_B \underline{\nabla} T + S(t) e^{-k^2(t) r^2} \qquad \text{(A1)}$$

whre κ and the Gaussian energy deposition term, $S(t)e^{-k^2r^2}$, have already been discussed. The other equation required is the continuity equation,

$$\frac{1}{\rho} \frac{d\rho}{dt} = -\underline{\nabla} \cdot \underline{v} \quad . \qquad \text{(A2)}$$

Assuming $dP/dt \approx 0$, Eq. (A1) gives an algebraic equation for $\underline{\nabla} \cdot \underline{v}$ which may be combined with Eq. (A2) to give

$$\frac{1}{T} \frac{dT}{dt} = \frac{S(t)}{P_\infty \gamma} e^{-k^2(t) r^2} + \underline{\nabla} \cdot \frac{\kappa}{T} \underline{\nabla} T \qquad \text{(A3)}$$

where P_∞ is the background pressure. The solution is then

$$T(r,t) = T_\infty e^{A(t) e^{-k^2(t) r^2}} \qquad \text{(A4)}$$

and

$$\rho(r,t) = \rho_\infty e^{-A(t) e^{-k^2(t) r^2}} \qquad \text{(A5)}$$

where T_∞ and ρ_∞ are the background temperature and density, respectively. Thus the nonlinear slow flow equations including expansions and contractions of the flow have been converted into a single equation which is linear in the logarithm of the temperature.

The total energy of the system at any instant is the sum of the internal energy and the work performed in expanding the heated region. It may be written

$$E(t) = \frac{P_\infty \gamma}{\gamma-1} \int_0^\infty 4\pi r^2 dr \left[1 - \frac{\rho(r,t)}{\rho_\infty}\right] \tag{A6}$$

$$= \frac{\gamma P_\infty}{(\gamma-1)k^3(t)} \int_0^\infty 4\pi x^2 \left[1-e^{-Ae^{-x^2}}\right] dx$$

$$\equiv \frac{\gamma P_\infty}{(\gamma-1)\ k^3(t)} F(A(t)). \tag{A7}$$

which defines the integral F(A(t)). Differentiating this we find that

$$\frac{dE}{dt} = \frac{\pi^{3/2} S(t)}{(\gamma-1)k^3(t)} \tag{A8}$$

which may be equated to

$$\frac{dE}{dt} = \frac{\partial E}{\partial k}\frac{\partial k}{\partial t} + \frac{\partial E}{\partial A}\frac{\partial A}{\partial t}. \tag{A9}$$

Thus a consistency condition has been specified on the rates of change of the amplitude, A(t), and the scale size $k^{-1}(t)$ for the heated region.

If the fluid velocity v is then expanded such that

$$v(r) \approx v_1(t)\ r, \tag{A10}$$

that is, only the linear term is kept, two coupled ordinary differential equations for k and A may be obtained,

$$\frac{dk}{dt} = -kv_1 - 2\kappa k^3 \tag{A11}$$

$$\frac{dA}{dt} = \frac{S(t)}{\gamma P} - 6\kappa k^2 A. \tag{A12}$$

Then the expression for v_1 may be written in terms of the integral F(A)

$$v_1 = \frac{S}{3\gamma P_\infty} \frac{F'(0) - F'(A)}{F(A)} + 2\kappa k^2 \frac{AF'(A) - F(A)}{F(A)} \tag{A13}$$

which results from using the principle of energy conservation and equating Eqs. (A8) and (A9).

EFFECT OF RADIATIVE LOSSES

When a large amount of energy is deposited in a small volume, the effect of radiative losses may be significant. Exact calculation of all the low temperature radiation effects is still beyond even the best detailed calculations today. An idealized model can be included in the similarity solution, however, to estimate these effects.

Black body radiation from a spherical surface at radius r takes energy out of the system at a rate

$$\frac{dE_{rad}}{dt} = 4\pi r^2 \sigma T^4(r). \tag{A14}$$

In the similarity solution the temperature at any radius r is given by

$$T(r, t) = T_\infty \; e^{A(t)e^{-k^2(t)r^2}} . \tag{A15}$$

Therefore,

$$\frac{dE_{rad}}{dt} = 4\pi\sigma T_\infty^4 \; r^2 \; e^{4A(t)e^{-k^2(t)r^2}} . \tag{A16}$$

However at t = 0 (A = 0),

$$\frac{dE_{rad}}{dt} = 0 . \tag{A17}$$

Therefore the background radiation into the volume must be substracted from (A 16) to give

$$\frac{dE_{rad}}{dt} = 4\pi\sigma T_\infty^4 \; r^2 e^{4A(t)e^{-h^2(t)^2}} - 4\pi\sigma T_\infty^4 \; r^2 . \tag{A18}$$

The next step is to choose r such that Eq. A18 is maximized. By assuming that the loss from the system proceeds at the maximum rate possible, the model is sure to signal the onset of radiative loss effects at least as soon as they occur in the physical system itself.

REFERENCES

1. Oran, E. S., and Boris, J. P., Prog. Energy Combustion Science. 7:1-72 (1981).
2. Oran, E. S., and Boris, J. P., presented at the 7th International Colloquium on Gas Dynamics of Explosions and Reactive Systems, Göttingen, 1979.
3. Lewis, B., and von Elbe, G., Combustion, Flames and Explosions of Gases, Academic Press, New York, San Francisco, London, 1961, pp. 323-367.
4. Weinberg, F. J., and Wilson, J. R., Proc. R. Soc. Lond. A321, 41-52 (1971).
5. Kingdon, R. G., and Weinberg, F. J., Sixteenth Symposium (International) on Combustion, The Combustion Institute, Pittsburgh, 1977, p. 747.
6. Dixon-Lewis, G., and Shepherd, I. G., Fifteenth Symposium (International) on Combustion, The Combustion Institute, Pittsburgh, 1975, p. 1483.
7. Dixon-Lewis, G., Combustion Flame 33, 319-321 (1978).
8. Overley, J. R., Overholser, K. A., and Reddien, G. W., Combustion Flame 31, 69-83 (1978).
9. Ballal, D. R., and Lefebvre, A. H., Proc. R. Soc. Lond. A357, 163-181 (1977).
10. Williams, F. A., Combustion Theory, Addison Wesley, Reading, Palo Alto, London, 1965, p. 2.
11. Boris, J. P., ADINC: An Implicit Lagrangian Hydrodynamics Code, N.R.L. Memorandum Report 4022, Naval Research Laboratory, Washington, D.C., 1979.
12. Jones, W. W., and Boris, J. P., Flame - A Slow Flow Combustion Model, N.R.L. Memorandum Report 3790, Naval Research Laboratory, Washington, D.C., 1979.
13. Burks, T. L., and Oran, E. S., A Computational Study of the Chemical Kinetics of Hydrogen Combustion, N.R.L. Memorandum Report 4446, Naval Research Laboratory, Washington, D.C., 1980.
14. Stull, D. R., and Prophet, H., JANAF Thermochemical Tables, National Standard Reference Data Series, U. S. National Bureau of Standards, No. 37, 2nd Ed., Gaithersburg, Maryland, 1971.

15. Young, T. R., and Boris, J. P., J. Phys. Chem. 81, 2424-2427 (1977).

16. Young, T. R., CHEMEQ, A Subroutine for Solving Stiff Ordinary Differential Equations, N.R.L. Memorandum Report 4091, Naval Research Laboratory, Washington, D.C., 1980.

17. Jones, W. W., and Boris, J. P., J. Phys. Chem. 81, 2532-2534 (1977).

18. Oran, E. S., Boris, J. P., Young, T. R., Flanigan, M., Burks, T., and Picone, M., Eighteenth Symposium (International) on Combustion, The Combustion Institute, Pittsburgh, 1981.

19. Mason, E. A., and Saxena, S.C., Phys. Fluids 1, 361-369 (1958).

20. Blanc, M. V., Guest, P. G., von Elbe, G., and Lewis, B., J. Chem. Phys. 15, 798-802 (1947).

21. Lewis, B., and von Elbe, G., Combustion, Flame and Explosions of Gases, Academic Press, New York, San Francisco, London, 1961, p. 326.

22. Taki, S., and Fujiwara, T., Proc. AIAA 9th Fluid and Plasma Dynamics Conference, 1-9 (1976).

23. Kailasanath, K., Oran, E.S., Boris, J.P., and Young, T.R., A One-Dimensional Time-Dependent Model For Flame Initiation, Propagation and Quenching, to be published as N.R.L. Memorandum Report, Naval Research Laboratory, Washington, D.C., 1981.

24. Baulch, D.L., Drysdale, D.C., Horne, D.G., and Lloyd, A.C., Evaluated Kinetic Data for High Temperature Reactions, Vol. 1, Butterworths, London, 1972.

25. Hampson, R.F., and Garvin, D., "Chemical Kinetic and Photochemical Data for Modelling of Atmospheric Chemistry," NBS Technical Note 866, National Bureau of Standards, Washington, D.C. (1975).

26. Choen, N., and Westberg, K.R., "Data Sheets," The Aerospace Corporation, P.O. Box 92957, Los Angeles, California (1979).

27. Olson, D.B., and Gardiner, W.C., J. Phy. Chem., 81, 2514 (1977).

28. Lloyd, A.C., Int. J. Chem. Kinetics, 6 169 (1974).

29. Bahn, G.S., "Reaction Rate Compilation for H-O-N System," Gordon and Breach, New York, 1968.

Table I. H_2-O_2 Elementary Reactive Mechanism

Reaction	$k_i = AT^B \exp(-C/T)$[a] A[b]	B	C[b]	Reference
$H + HO \rightleftarrows O + H_2$	1.40(-14)	1.00	3.50(+03)	[24]
	3.00(-14)	1.00	4.48(+03)	[24]
$H + HO_2 \rightleftarrows H_2 + O_2$	4.20(-11)	0.00	3.50(+02)	[24]
	9.10(-11)	0.00	2.91(+04)	[24]
$H + HO_2 \rightleftarrows HO + HO$	4.20(-10)	0.00	9.50(+02)	[24]
	2.00(-11)	0.00	2.02(+04)	[24]
$H + HO_2 \rightleftarrows O + H_2O$	8.30(-11)	0.00	5.00(+02)	[25]
	1.75(-12)	0.45	2.84(+04)	$k_r = k_f/K_c$
$H + H_2O_2 \rightleftarrows HO_2 + H_2$	2.80(-12)	0.00	1.90(+03)	[24]
	1.20(-12)	0.00	9.40(+03)	[24]
$H + H_2O_2 \rightleftarrows HO + H_2O$	5.28(-10)	0.00	4.50(+03)	[24]
	3.99(-10)	0.00	4.05(+04)	$k_r = k_f/K_c$
$HO + H_2 \rightleftarrows H + H_2O$	1.83(-15)	1.30	1.84(+03)	[26]
	1.79(-14)	1.20	9.61(+03)	[26]
$HO + HO \rightleftarrows H_2 + O_2$	1.09(-13)	0.26	1.47(+04)	$k_f = k_r/K_c$
	2.82(-11)	0.00	2.42(+04)	[27]
$HO + HO \rightleftarrows O + H_2O$	1.00(-16)	1.30	0.00(+00)	[26]
	3.20(-15)	1.16	8.77(+03)	$k_r = k_f/K_c$
$HO + HO_2 \rightleftarrows H_2O + O_2$	8.30(-11)	0.00	5.03(+02)	[28]
	2.38(-10)	0.17	3.69(+04)	$k_r = k_f/K_c$
$HO + H_2O \rightleftarrows HO_2 + H_2$	1.70(-11)	0.00	9.10(+02)	[24]
	4.70(-11)	0.00	1.65(+04)	[24]
$HO + O_3 \rightleftarrows HO_2 + O_2$	1.60(-12)	0.00	9.56(+02)	[25]
	6.69(-14)	0.33	2.04(+04)	$k_r = k_f/K_c$
$HO + H_2 \rightleftarrows HO + H_2O$	1.20(-12)	0.00	9.41(+03)	[27]
	1.33(-14)	0.43	3.62(+04)	$k_r = k_f/K_c$
$HO_2 + HO_2 \rightleftarrows H_2O_2 + O_2$	3.00(-11)	0.00	5.00(+02)	[25]
	1.57(-09)	-0.38	2.20(+04)	$k_r = k_f/K_c$

Table I. (continued)

H_2-O_2 Elementary Reactive Mechanism

Reaction	$k_i = AT^B \exp(-C/T)$ [a]			Reference
	A [b]	B	C [b]	
$O + HO \rightleftarrows H + O_2$	2.72(-12)	0.28	-8.10(+01)	$k_f = k_r/K_c$
	3.70(-10)	0.00	8.45(+03)	[24]
$O + HO_2 \rightleftarrows HO + O_2$	8.32(-11)	0.00	5.03(+02)	[28]
	2.20(-11)	0.18	2.82(+04)	$k_r = k_f/K_c$
$O + H_2O_2 \rightleftarrows H_2O + O_2$	1.40(-12)	0.00	2.12(+03)	[25]
	5.70(-14)	0.52	4.48(+04)	$k_r = k_f/K_c$
$O + H_2O_2 \rightleftarrows HO + HO_2$	1.40(-12)	0.00	2.13(+03)	[25]
	2.07(-15)	0.64	8.23(+03)	$k_r = k_f/K_c$
$H + H + M \rightleftarrows H_2 + M$	1.80(-30)	-1.00	0.00(+00)	[24]
	3.70(-10)	0.00	4.83(-04)	[24]
$H + HO + M \rightleftarrows H_2O + M$	6.20(-26)	-2.00	0.00(+00)	[24]
	5.80(-09)	0.00	5.29(+04)	[24]
$H + O_2 + M \rightleftarrows HO_2 + M$	4.14(-33)	0.00	-5.00(+02)	[24]
	3.50(-09)	0.00	2.30(+04)	[24]
$HO + HO + M \rightleftarrows H_2O_2 + M$	2.50(-33)	0.00	-2.55(+03)	[24]
	2.00(-07)	0.00	2.29(+04)	[24]
$O + H + M \rightleftarrows HO + M$	8.28(-29)	-1.00	0.00(+00)	[29]
	2.33(-10)	0.21	5.10(+04)	$k_r = k_f/K_c$
$O + HO + M \rightleftarrows HO_2 + M$	2.80(-31)	0.00	0.00(+00)	[29]
	1.10(-04)	-0.43	3.22(+04)	$k_r = k_f/K_c$
$O + O + M \rightleftarrows O_2 + M$	5.20(-35)	0.00	-9.00(+02)	[24]
	3.00(-06)	-1.00	5.94(+04)	[24]

(a) Bimolecular reaction rate constants are given in units of $cm^3/(molecule\ sec)$. Termolecular reaction rate constants are given in units of $cm^6/(molecule^2\ sec)$.

(b) Exponentials to the base 10 are given in parenthesis; i.e., 1.00(-10) = 1.00×10^{-10}.

Table II

Case	Initial Radius of Deposition R_o (cm)	Total Energy Deposited E_o (mJ)	Ignition Prediction	
			Detailed Numerical Simulation	Similarity Solution
1	0.1	4.0	yes	yes
		3.7	yes	yes
		3.0	no	no
2	0.11	5.0	yes	yes
		3.0	no	no
3	0.12	7.0	yes	yes
		6.0	no	no
4	0.09	3.3	no	yes
5	0.08	3.3	no	yes

FIGURE CAPTIONS

Figure 1 Time history of the temperature profile in a $H_2:O_2:N_2$/ 2:1:10 mixture as predicted by the detailed numerical simulation model.

Figure 2 Temperature as a function of induction time for $H_2:O_2:N_2$/2:1:10 mixture evaluated using the chemical reaction scheme in Table I.

Figure 3 The nonlinear amplitude, A, and the characteristic radius, R_c, as functions of time calculated using the similarity solution model.

Figure 4 Calculations of the central temperature as a function of time for three values of E_o using the detailed numerical simluation model.

Figure 5 The central temperature as a function of time for three values of E_o as predicted by the similarity solution model.

Figure 6 Calculations of the induction parameter as a function of time for three values of E_o using the similarity solution model. The "*" indicates the predicted time of ignition.

Figure 7 Comparisons of the time history of the temperature profiles predicted by the detailed numerical model and the similarity solution model.

Figure 8 The minimum ignition energy as a function of the radius of energy deposition calculated using detailed numerical simulations.

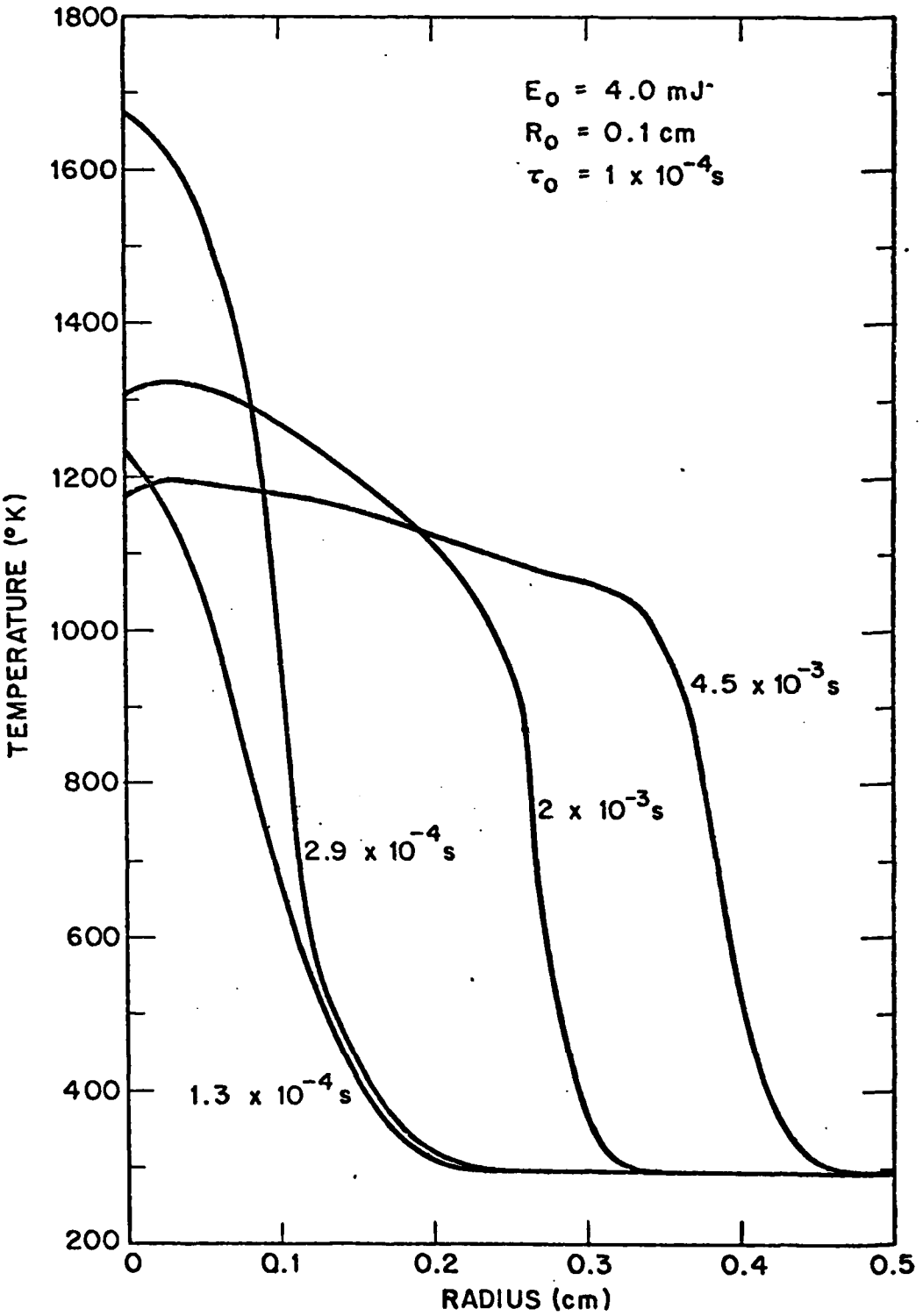
1800
1600
1400
1200
1000
800
600
400
200
TEMPERATURE (°K)
0
0.1
0.2
0.3
0.4
0.5
RADIUS (cm)
E_o = 4.0 mJ
R_o = 0.1 cm
τ_o = 1 x 10^{-4}s
4.5 x 10^{-3}s
2 x 10^{-3}s
2.9 x 10^{-4}s
1.3 x 10^{-4}s

Figure 1

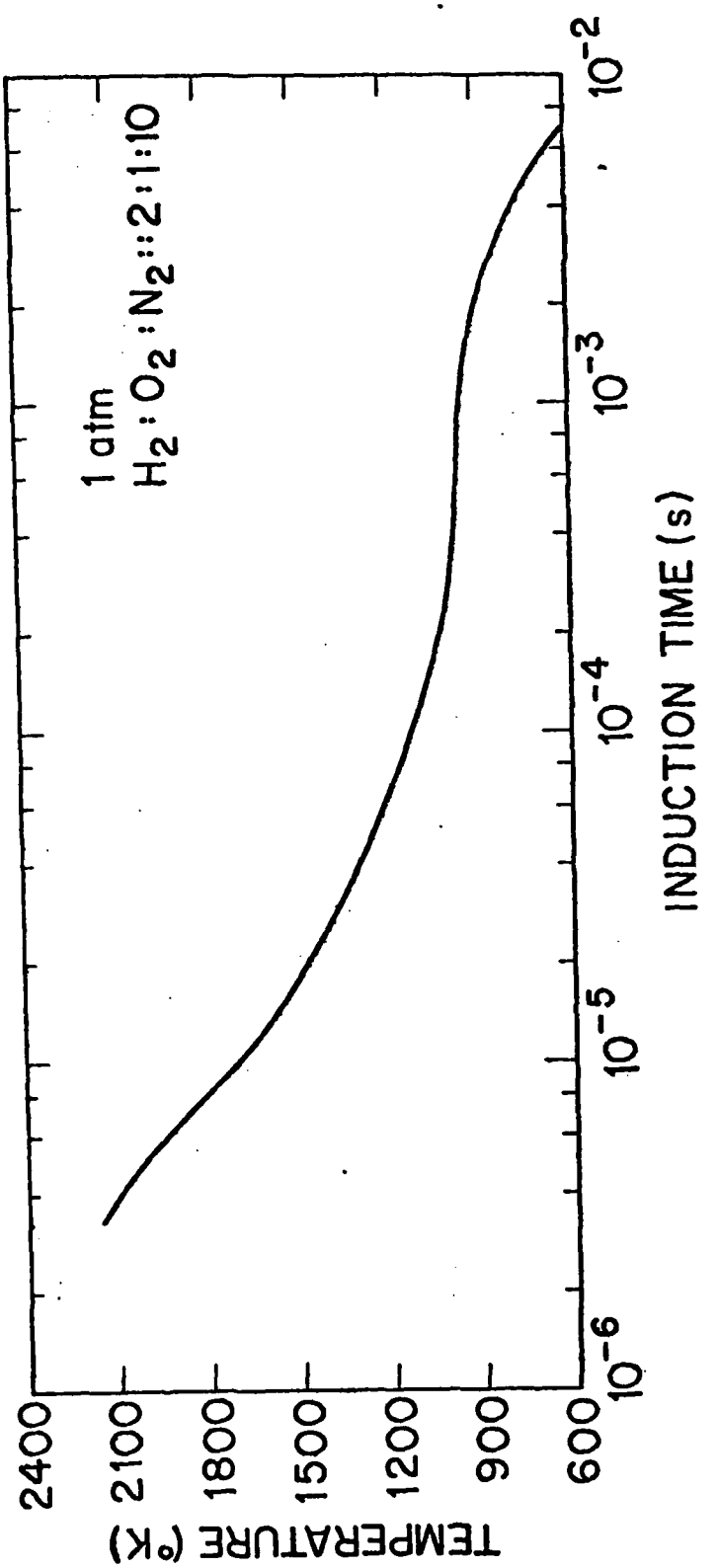
1 atm
$H_2 : O_2 : N_2 :: 2 : 1 : 10$
TEMPERATURE (°K)
2400
2100
1800
1500
1200
900
600
10^{-6}
10^{-5}
10^{-4}
10^{-3}
10^{-2}
INDUCTION TIME (s)

Figure 2

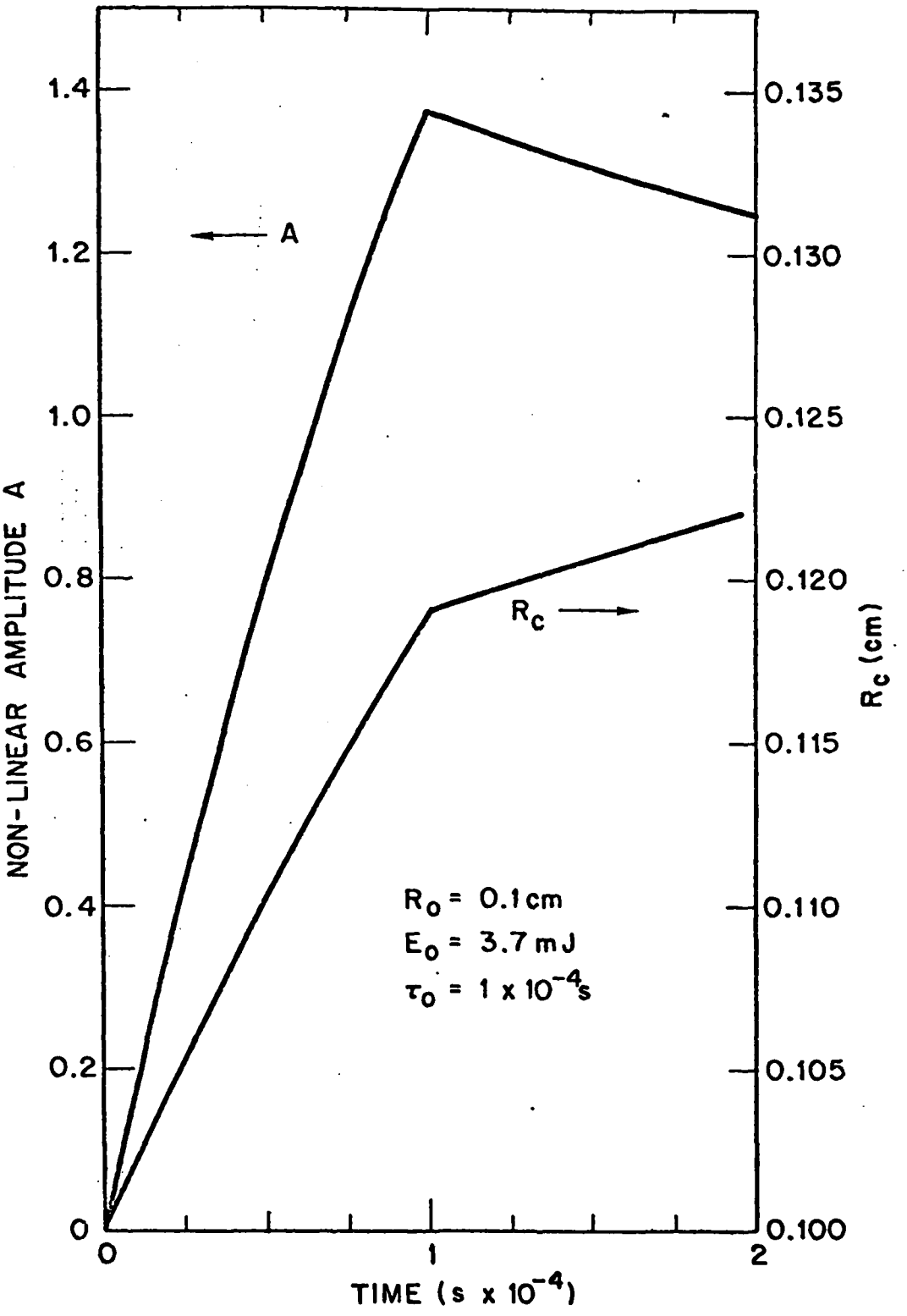
1.4
1.2
1.0
0.8
0.6
0.4
0.2
0
0.135
0.130
0.125
0.120
0.115
0.110
0.105
0.100
A
R_c
R_c (cm)
NON-LINEAR AMPLITUDE A
R_0 = 0.1 cm
E_0 = 3.7 mJ
τ_0 = 1 x 10^{-4} s
0
1
2
TIME (s x 10^{-4})

Figure 3

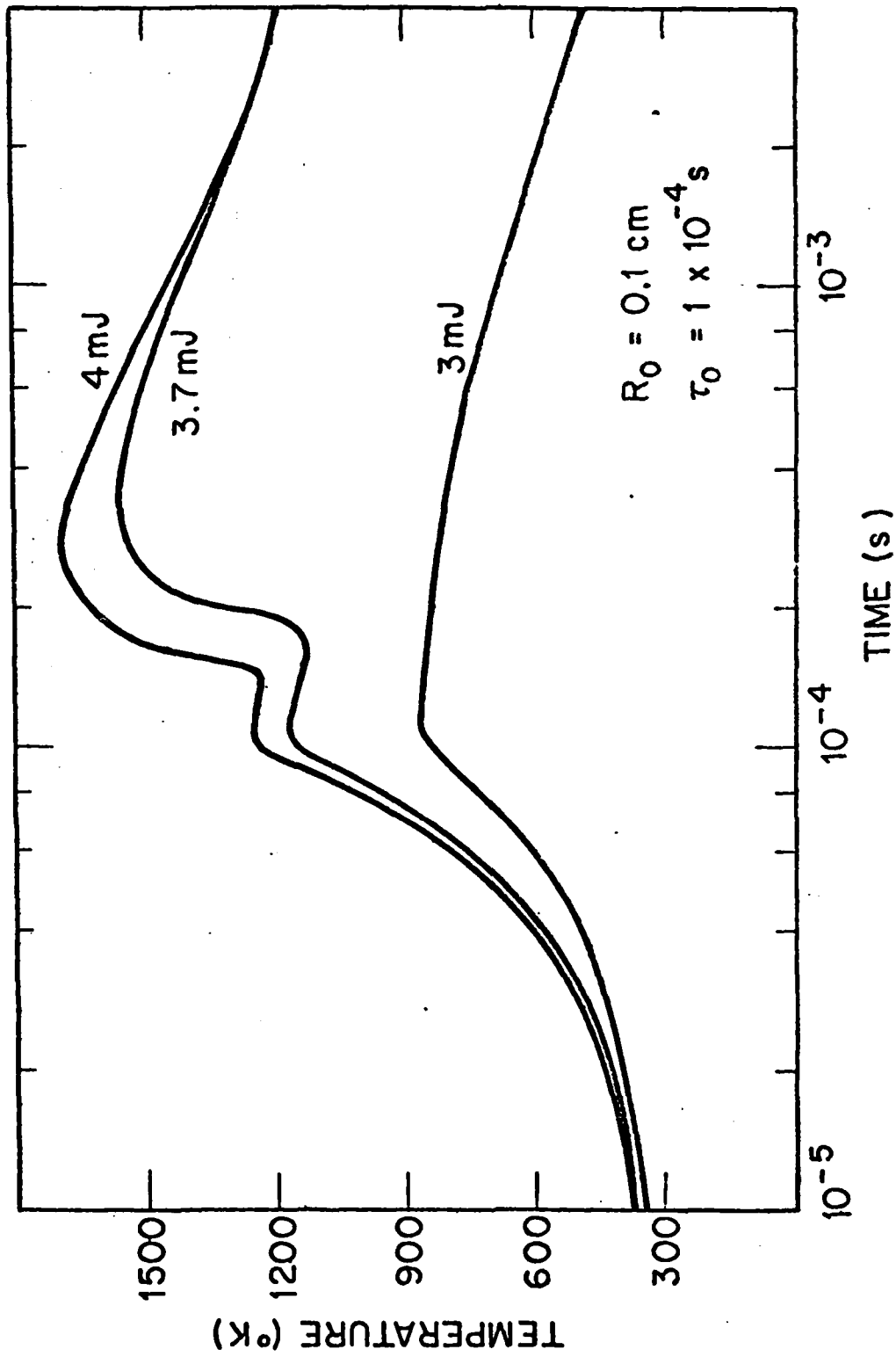
4 mJ
3.7 mJ
3 mJ
R_0 = 0.1 cm
τ_0 = 1 x 10^{-4} s
10^{-5}
10^{-4}
10^{-3}
TIME (s)
1500
1200
900
600
300
TEMPERATURE (°K)

Figure 4

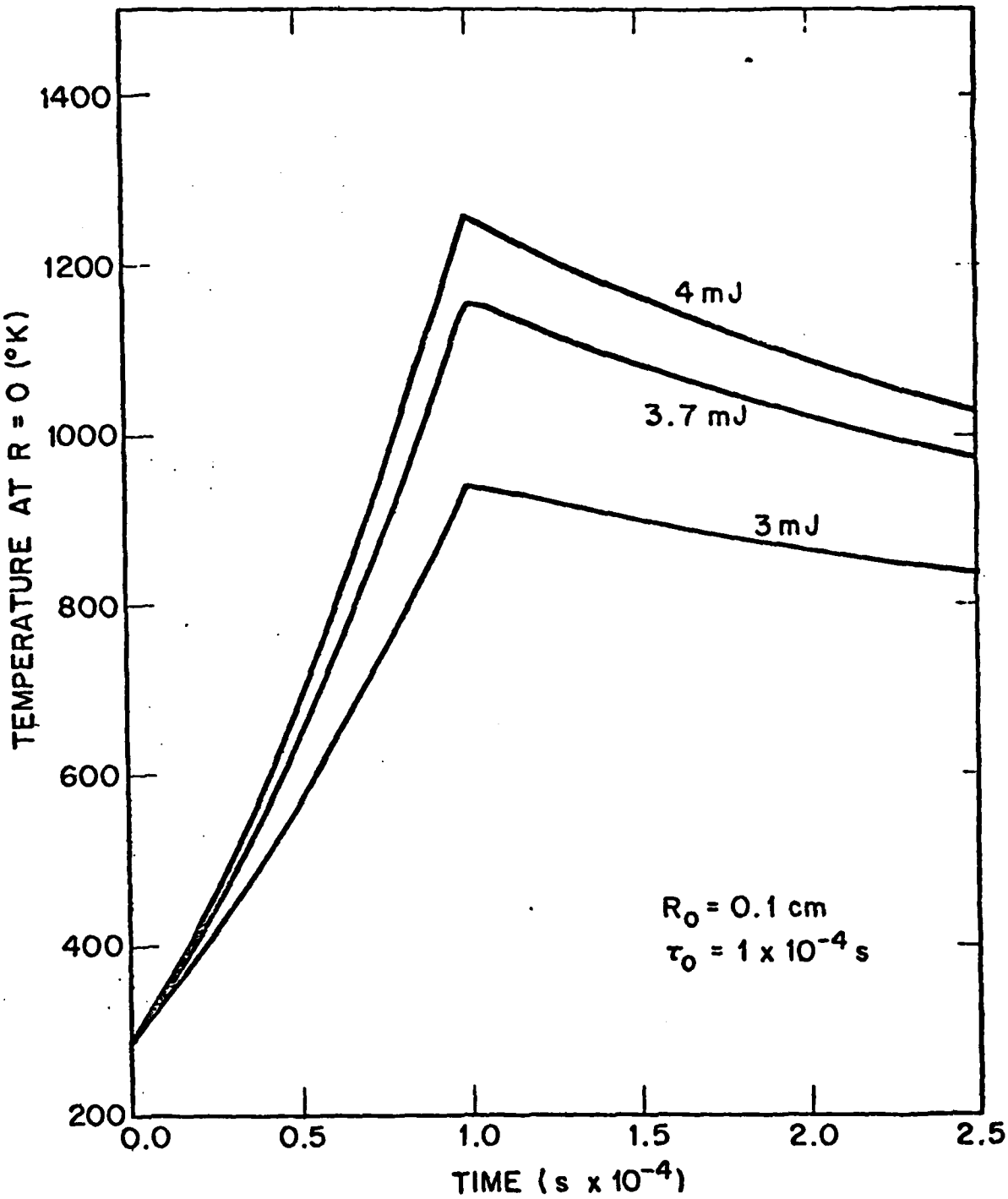
1400
1200
1000
800
600
400
200
TEMPERATURE AT R = 0 (°K)
4 mJ
3.7 mJ
3 mJ
R_0 = 0.1 cm
τ_0 = 1 x 10^{-4} s
0.0
0.5
1.0
1.5
2.0
2.5
TIME (s x 10^{-4})

Figure 5

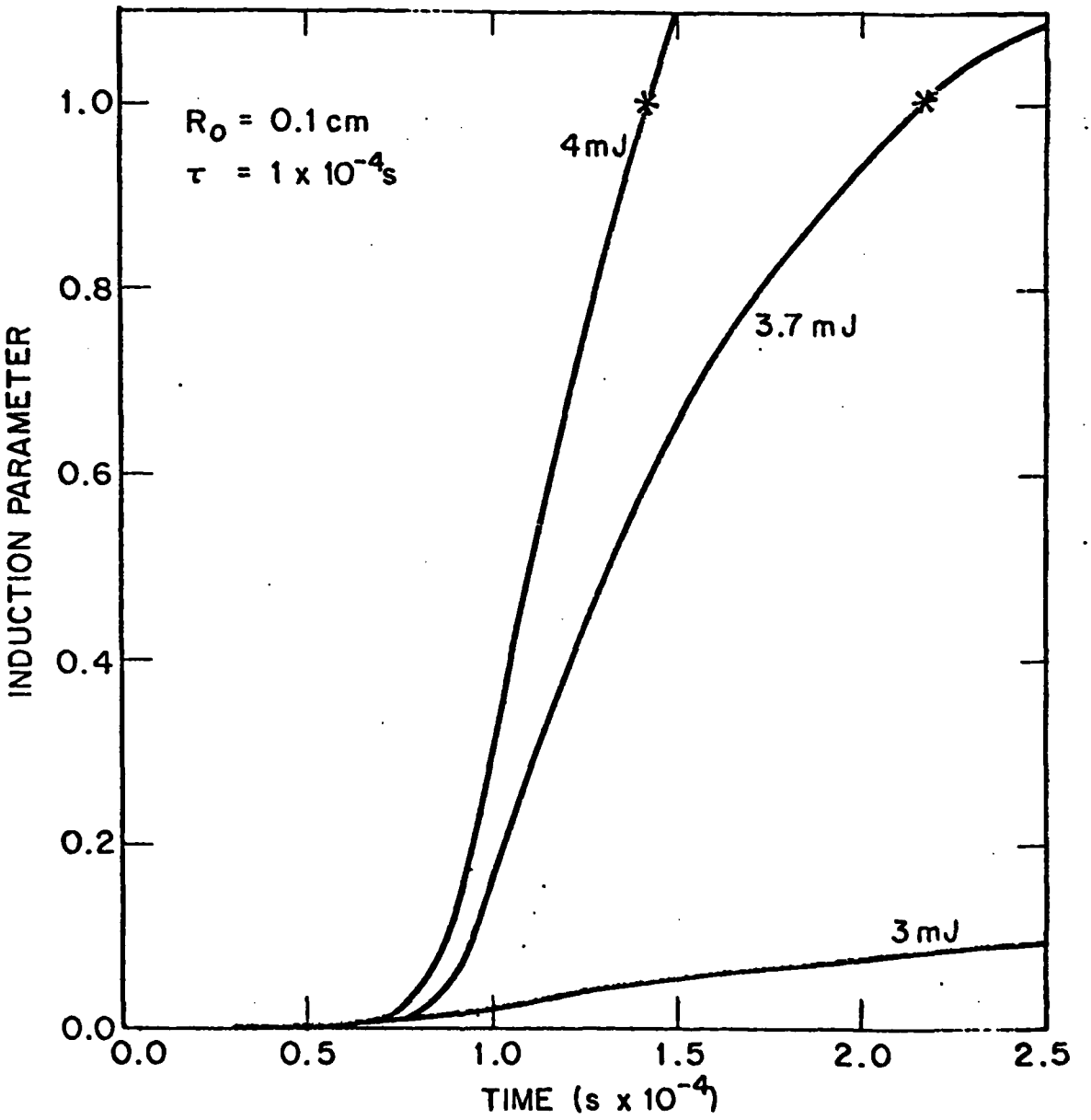
R_o = 0.1 cm
τ = 1 x 10^{-4}s
4 mJ
3.7 mJ
3 mJ
INDUCTION PARAMETER
TIME (s x 10^{-4})
0.0
0.2
0.4
0.6
0.8
1.0
0.0
0.5
1.0
1.5
2.0
2.5

Figure 6

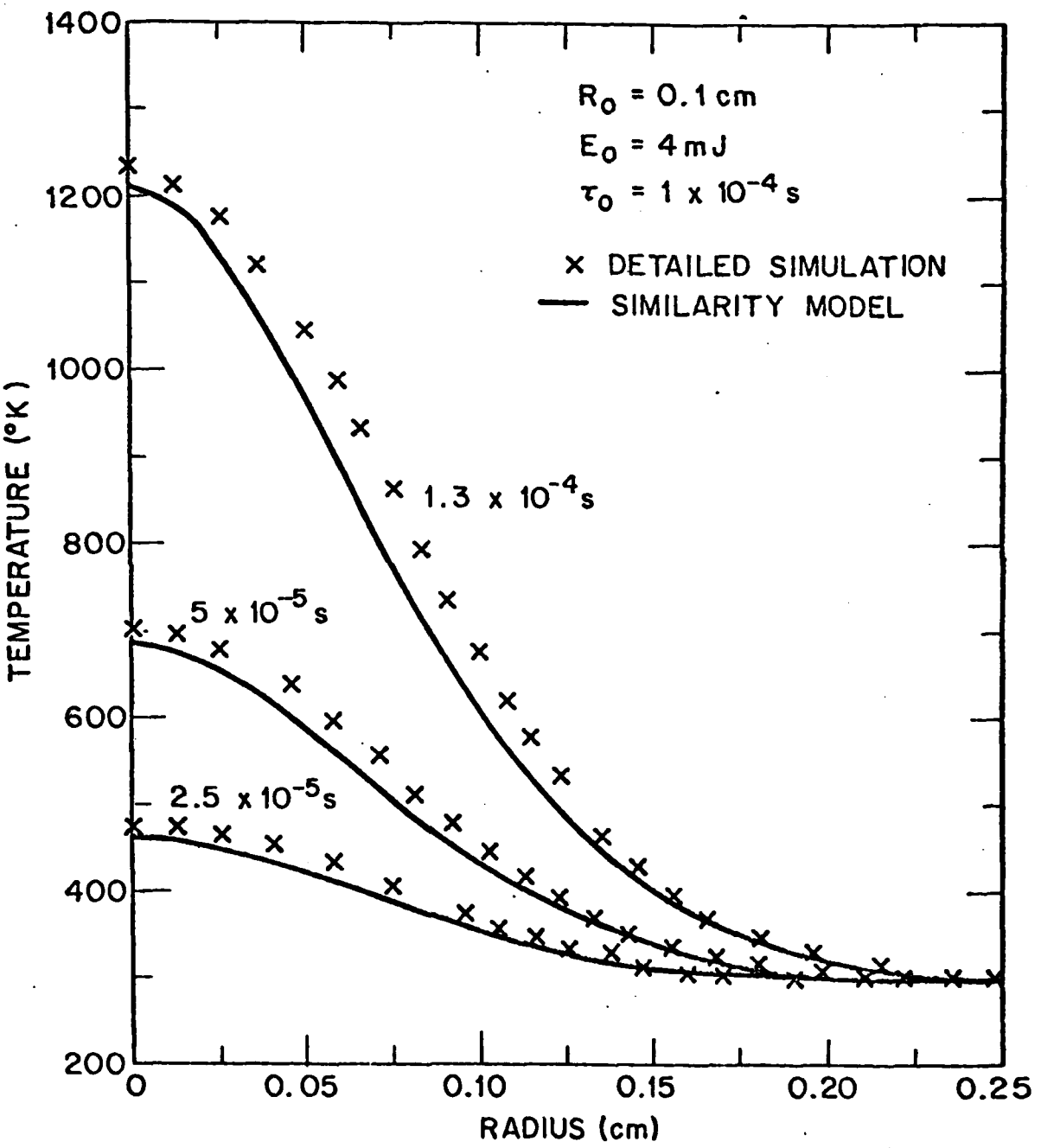
1400
1200
1000
800
600
400
200
TEMPERATURE (°K)
0
0.05
0.10
0.15
0.20
0.25
RADIUS (cm)
R_0 = 0.1 cm
E_0 = 4 mJ
τ_0 = 1 x 10^{-4} s
× DETAILED SIMULATION
— SIMILARITY MODEL
1.3 x 10^{-4}s
5 x 10^{-5}s
2.5 x 10^{-5}s

Figure 7

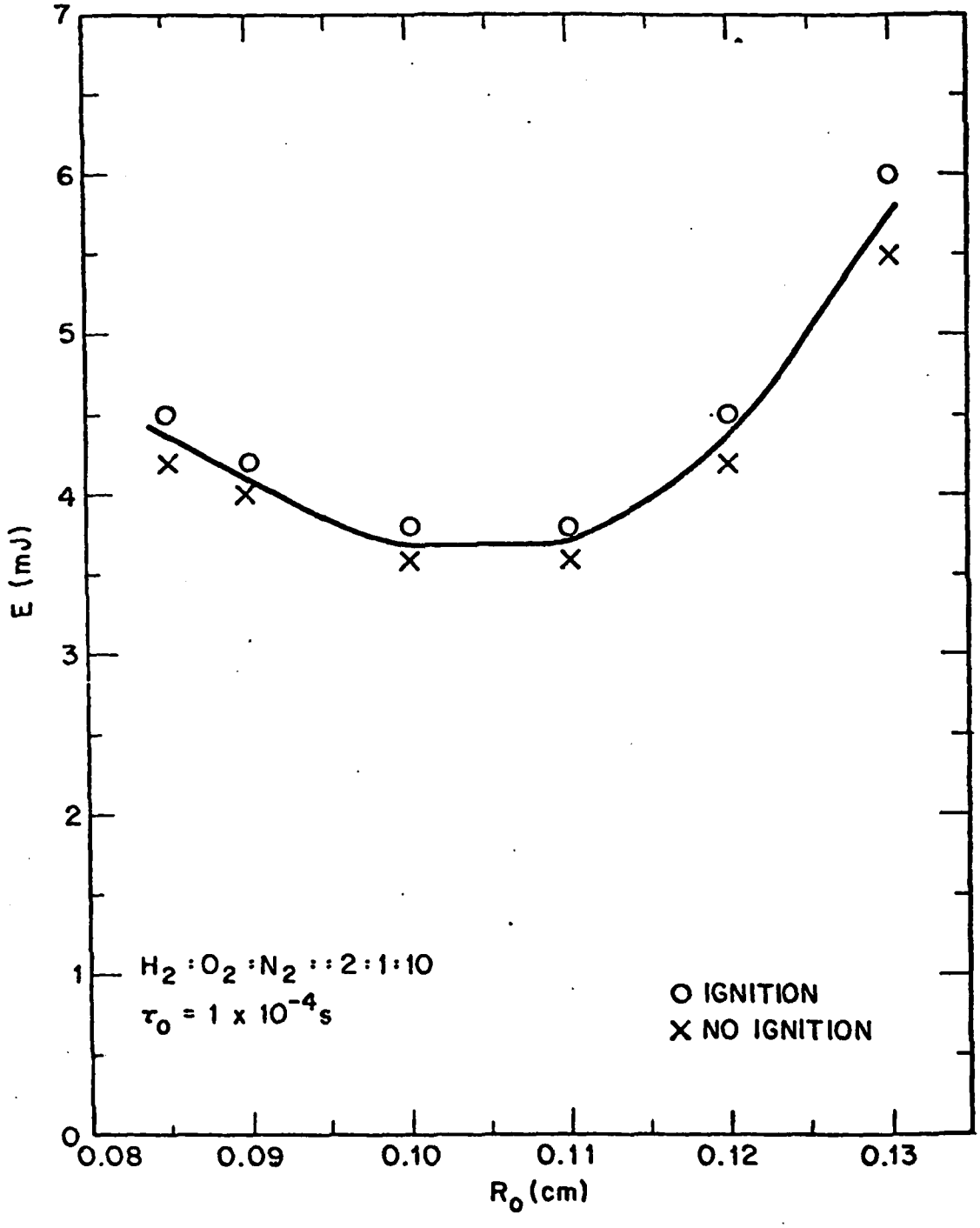
7
6
5
4
3
2
1
0
E (mJ)
0.08
0.09
0.10
0.11
0.12
0.13
R_0 (cm)
$H_2 : O_2 : N_2 :: 2 : 1 : 10$
$\tau_0 = 1 \times 10^{-4}$s
O IGNITION
X NO IGNITION

Figure 8

Appendix C

REVISED SUBROUTINES - INITAL AND RTCON

```
..PRINT TEMP

*** MEMBER INITAL     OLD DATE = 81.342   TIME = 10:28   CHECKSUM = 2FB81B88

      1*          SUBROUTINE  INITAL
      2* C        ----------  ------
      3* C
      4* C***  INITIALIZE EVERYTHING IN SIGHT  ***
      5* C
      6* C        THE ORDER OF INPUT ITEMS IS
      7* C
      8* C        1) NAMELIST  "SOLARP"
      9* C
     10* C             INPUT DATA WHICH DESCRIBE THE JACCHIA MODEL OF THE
     11* C             MAJOR NEUTRAL ATMOSPHERE
     12* C
     13* C             FBAR
     14* C             F
     15* C             DAY
     16* C             KP
     17* C             TINF
     18* C             MAT
     19* C             FCN
     20* C             FCN2
     21* C             FCN2
     22* C             FUVEQ
     23* C
     24* C        2) NAMELIST  "CNTS"
     25* C
     26* C             IONS          THE NUMBER OF ION SPECIE
     27* C             MINORS        THE NUMBER OF MINOR NEUTRAL SPECIE
     28* C             NZ            THE NUMBER OF GRID POINTS IN ALTITUDE
     29* C             ZBOT          THE BOTTOM OF THE MESH (LOWEST ALTITUDE IN KM)
     30* C             ZTOP          THE TOP OF THE MESH (HIGHEST ALTITUDE IN KM)
     31* C             DZ0           THE SPACING BETWEEN THE TWO LOWEST GRID
     32* C                           POINTS IN ALTITUDE
     33* C             ZPLOT         THE ALTITUDE AT WHICH TIME PLOTS ARE TO BE
     34* C                           MADE (IN KM)
     35* C             DT            THE TIME STEP (IN SECONDS)
     36* C             MODA          MAGNETIC DIP ANGLE (IN DEGREES)
     37* C             LAT           THE (IN DEGREES) LATITUDE
     38* C             DGRADA        THE STEP SIZE IN LATITUDE FOR COMPUTATION
     39* C                           OF PRESSURE GRADIENTS (IN DEGREES) --
     40* C                           DEFAULT: 10.0
     41* C             WDHA          PHASE FACTOR FOR NEUTRAL WINDS
     42* C                           DEFAULT: 0.0
     43* C             PGSFI         PRESSURE GRADIENT SCALE FACTOR  --
     44* C                           DEFAULT: 1.0
     45* C             EEFX          ELECTRON HEATING EFFICIENCY SCALE FACTOR --
     46* C                           DEFAULT: 1.0
     47* C             FLUXF         DAYTIME SOLAR FLUX SCALE FACTOR  --
     48* C                           DEFAULT: 1.0
     49* C             JAX1          THE MAXIMUM NUMBER OF INTERVALS FOR THE
```

*** MEMBER INITAL OLD DATE = 81,342 TIME = 10:24 CHECKSUM = 2FD01BD8

```
C                     MASS INTEGRAL INTEGRATION IN THE THE
C                     DEPOSITION RATE CALCULATION AT ZBOT
C        JAXP         THE MAXIMUM NUMBER OF INTERVALS FOR THE
C                     MASS INTEGRAL INTEGRATION IN THE
C                     DEPOSITION RATE CALCULATION AT ZTOP
C
C     3) NAMELIST  "CTRL"
C
C        MAXSTP       THE MAXIMUM STEP THE PROGRAM WILL COMPUTE
C        NDAY         THE MAXIMUM DAY TO WHICH TO COMPUTE
C        NHMAX        THE MAXIMUM HOUR IN THE MAXIMUM DAY TO
C                     WHICH TO COMPUTE
C        IAUPT        THE NUMBER OF TIME STEPS BETWEEN COMPUTATIONS
C                     OF THE MAJOR NEUTRAL DENSITIES --
C                     DEFAULT: 2
C        IPEP         THE NUMBER OF TIME STEPS BETWEEN COMPUTATIONS
C                     OF THE DEPOSITION RATES -- DEFAULT: 2
C        ICHEM        A LOGICAL VARIABLE, .TRUE. IF CHEMISTRY
C                     IS TO BE DONE -- DEFAULT: .TRUE.
C        TRNP         A LOGICAL VARIABLE, .TRUE. IF TRANSPORT
C                     IS TO BE DONE -- DEFAULT: .TRUE.
C        LINDR        THE INPUT UNIT NUMBER FOR THE DEPOSITION
C                     INFORMATION -- DEFAULT: 5
C        LOTDR        THE OUTPUT UNIT NUMBER
C        LPRIC        A LOGICAL VARIABLE, .TRUE. IF A PRINTOUT
C                     OF THE INPUT TO THE CHEMISTRY AND
C                     DEPOSITION ROUTINES IS DESIRED --
C                     DEFAULT: .TRUE.
C        RSTART       A LOGICAL VARIABLE, .TRUE. IF THIS IS A
C                     CONTINUATION OF A PREVIOUS RUN --
C                     DEFAULT: .FALSE.
C        LDDMP        AN OUTPUT UNIT NUMBER FOR DUMPS TO DISK
C                     FOR RESTART PURPOSES
C        LTDMP        AN OUTPUT UNIT NUMBER FOR DUMPS TO TAPE
C        TDUMP        THE NUMBER OF TIME STEPS BETWEEN DUMPS
C                     TO TAPE
C        DDUMP        THE NUMBER OF TIME STEPS BETWEEN DUMPS
C                     TO DISK
C
C     4) NSYMPL AND RELATED DATA
C
C        THE DATA CARDS FOR IONS SHOULD PRECEDE THOSE FOR THE
C        MINOR NEUTRALS WHICH PRECEDE THOSE FOR THE FIVE (5)
C        MAJOR NEUTRALS AND FINALLY THE ELECTRON. EACH CARD
C        CONSISTS OF THE FOLLOWING FIELDS:
C
C             COLUMNS
C              1 -  6  A SIX CHARACTER SYMBOL IDENTIFYING THE
C                      SPECIE (LEFT JUSTIFIED)
C              7 - 14  THE ATOMIC MASS OF THE SPECIE (F8.1)
```

*** MEMBER INITAL OLD DATE = 81.342 TIME = 10:24 CHECKSUM = 2FB41888

```
101* C                  15 - 17  THE TYPE OF BOUNDARY CONDITION FOR THE
102* C                           CONTINUITY EQUATION TO USE AT THE HIGH
103* C                           ALTITUDE (I3)
104* C                  18 - 25  THE HIGH ALTITUDE AT WHICH THE BOUNDARY
105* C                           CONDITION IS APPLIED (F8.1)
106* C                  26 - 33  FOR MINOR NEUTRALS, THE BOUNDARY VALUE (F8.1)
107* C                  34 - 41  FOR MINOR NEUTRALS, A DIFFUSION COEFFICIENT
108* C                           (F8.1)
109* C                  42 - 44  BLANK
110* C                  45       A OLE CHARACTER SYMBOL TO USE ON PLOTS TO
111* C                           IDENTIFY THIS SPECIE (A1)
112* C
113* C            THE LAST CARD IN THIS SECTION GIVES THE ORDER IN WHICH
114* C            THE CONTINUITY EQUATIONS ARE TO BE SOLVED WITH ALL THE
115* C            IONS DONE BEFORE ANY MINOR NEUTRAL
116* C
117* C
118* C        5) INITIAL PROFILES
119* C
120* C            FOR EACH ALTITUDE AT WHICH INITIAL CONDITIONS ARE KNOWN
121* C            THREE (3) CARDS ARE USED
122* C                 THE FIRST CARD GIVES THE ALTITUDE (Z), THE TWO
123* C                 COMPONENTS OF THE NEUTRAL WINDS (U,V), AND
124* C                 THE VIBRATIONAL ENERGY OF N2 (EVS).  (F8.1,7E8.1)
125* C                 THE SECOND CARD GIVES THE ION DENSITIES (8X,7E8.1)
126* C                 THE THIRD CARD GIVES THE MINOR NEUTRAL DENSITIES
127* C                 (8X,7E8.1)
128* C
129* C
130* C        6) OUTPUT CONTROL VARIABLES IN THE NAMELISTS
131* C                 IN SUBROUTINE  DSPLI
132* C
133* C            NAMELIST "PRTINP"
134* C
135* C              LU            A LOGICAL VARIABLE, .TRUE. IF THE
136* C                            HYDRODYNAMIC VARIABLES ARE TO BE PRINTED
137* C                            -- DEFAULT: .TRUE.
138* C              LV            A LOGICAL VARIABLE, .TRUE. IF THE ION
139* C                            VELOCITIES ARE TO BE PRINTED  --
140* C                            DEFAULT: .FALSE.
141* C              LC            A LOGICAL VARIABLE, .TRUE. IF THE
142* C                            CHEMISTRY VARIABLES ARE TO BE PRINTED  --
143* C                            DEFAULT: .TRUE.
144* C              LI            A LOGICAL VARIABLE, .TRUE. IF THE
145* C                            IONIZATION RATES OF NEUTRALS ARE TO BE
146* C                            PRINTED  --  DEFAULT: .FALSE.
147* C              LP            A LOGICAL VARIABLE, .TRUE. IF SELECTED
148* C                            PRODUCTION/LOSS RATES ARE TO BE PRINTED  --
149* C                            DEFAULT: .FALSE.
150* C              LPLT          A LOGICAL VARIABLE, .TRUE. IF PLOTS OF
151* C                            TEMPERATURES VS ALTITUDE ARE TO BE MADE  --
```

*** MEMBER INITAL PLD DATE = 81,342 TIME = 10:21 CHECKSUM = 2FB01888

```
152* C                              DEFAULT: .FALSE.
153* C           LPLD               A LOGICAL VARIABLE, .TRUE. IF PLOTS OF
154* C                              SELECTED DENSITIES VS ALTITUDE ARE TO BE
155* C                              MADE  --  DEFAULT: .FALSE.
156* C           ZRD(2)             THE MINIMUM AND MAXIMUM ALTITUDE COVERED
157* C                              IN THE PLOTS  --  DEFAULT: 100.0, 5000.0
158* C           LOGP               A LOGICAL VARIABLE, .TRUE. IF LOG-LOG
159* C                              PLOTS ARE DESIRED
160* C           PUNV(3)            THE HOUR, DAY, AND INCREMENT IN ALTITUDE
161* C                              INDEX AT WHICH TO PRODUCE PUNCHED OUTPUT
162* C                              FOR USE AS INITIAL CONDITIONS
163* C           PHRS(13)           SELECTED HOURS OF THE DAY AT WHICH
164* C                              PRINTED OUTPUT IS DESIRED
165* C           NPZPR              THE INCREMENT IN THE ALTITUDE INDEX FOR
166* C                              PRINTED OUTPUT
167* C           PHPDR              THE NUMBER OF HOURS BETEEN PRINTED OUTPUT
168* C           SPPHR              THE HOUR OF THE DAY THAT PRINTED OUTPUT
169* C                              IS TO START
170* C           SPPDY              THE DAY THAT PRINTED OUTPUT IS TO START
171* C           DIAG               A LOGICAL VARIABLE, .TRUE. IF PRINTED
172* C                              OUTPUT IS TO BE GENERATED AFTER EVERY STEP
173* C                              --  DEFAULT: .FALSE.
174* C
175* C       THE NEXT THREE ARE NOT CURRENTLY USED, THEY ARE ASSOCIATED
176* C         WITH MAKING PLOTS TO FILM WHICH HAS NOT BEEN IMPLEMENTED.
177* C
178* C           NFPLT
179* C           NPPLT
180* C           NSPLT
181* C
182* C
183* C           NAMELIST "RASTER"
184* C
185* C       OUTPUT VARIABLES FOR PLOTS TO FILM; NOT CURRENTLY USED
186* C
187* C           RASXDL
188* C           RASXDR
189* C           RASXTL
190* C           RASXTR
191* C           RASYSB
192* C           RASYST
193* C           XFRPRL
194* C           XFRPPR
195* C           XFRPBT
196* C           SPC
197* C           WPT
198* C           PGT
199* C
200* C
201* C       7) CHEMISTRY REACTION RATES
202* C                THROUGH SUBROUTINE  ARTP
```

*** MEMBER INITAL OLD DATE = 81,342 TIME = 10:24 CHECKSUM = 2F841B88

```
C
C       SEE "RTCON" FOR DESCRIPTION OF INPUT CARDS.
C
C    8) INITIALIZE DEPOSITION ROUTINES
C          THROUGH SUBROUTINE  DEPINT
C
C       NAMELIST "TOLDRH"
C
C       VARAIBLES USED TO MAKE A DEPOSITION TABLE, IF DESIRED.
C
C        LSPT          THE UNIT NUMBER OF THE FILE CONTAINING OR
C                      TO CONTAIN THE TABLE (SEE "MONTLU")
C        IDEPT         A TABLE IDENTIFIER -- DEFAULT: 0
C                      (DEFAULT GIVES NO TABLE  SEE "MONTLU")
C        MATE          THE JACCHIA MODEL TO USE FOR COMPUTING THE
C                      THE DEPOSITION TABLE
C        HRSMIN        THE MINIMUM HOUR IN THE TABLE --
C                      DEFAULT: 0.0
C        HRSMAX        THE MAXIMUM HOUR IN THE TABLE --
C                      DEFAULT: 24.0
C        NHRS          THE NUMBER OF TIME INTEVALS FOR THE TABLE
C                      -- DEFAULT: 96
C        ALTMIN        THE MINIMUM ALTITUDE IN THE TABLE --
C                      DEFAULT: ZBOT
C        ALTMAX        THE MAXIMUM ALTITUDE IN THE TABLE --
C                      DEFAULT: ZTOP
C        NALTS         THE NUMBER OF ALTITUDE INTERVALS IN THE
C                      TABLE -- DEFAULT: NZ-1
C        OPT(2)        THE TYPE OF GRID SPACING FOR THE TABLE.
C                      DEFAULT: 0, 1
C
C        THIS SECTION ALSO READS THE VARIOUS CROSS SECTIONS
C         FOR THE DAYTIME AND NIGHTTIME DEPOSITION
C
C
C
C***  THE  PROGRAM SIZE  ***
C
C   THE PARAMETERS:
C
C       NZ        THE MAXIMUM NUMBER OF GRID POINTS
C
C       MACTIV    THE MAXIMUM NUMBER OF ACTIVE SPECIES
C                       (IONS PLUS MINOR NEUTRALS)
C
C       MAXNS     THE MAXIMUM NUMBER OF SPECIES
C                       (NOT COUNTING ELECTRONS)
C
C       MR        THE MAXIMUM NUMBER OF CHEMICAL REACTIONS
```

```
*** MEMBER INITAL     OLD DATE = 81,342   TIME = 10:20   CHECKSUM = 2F801B08

C                              (INCLUDING DEPOSITION)
C
C       MDR       THE MAXIMUM NUMBER OF REACTIONS INVOLVING DEPOSITION
C
C       MP        THE MAXIMUM NUMBER OF REACTANTS PER REACTION
C
C   THE VARIABLES:
C
C       MZ        THE ACTUAL NUMBER OF GRID POINTS USED
C
C       IONS      THE ACTUAL NUMBER OF IONS
C
C       IONSP1    IONS  + 1
C
C       MINORS    THE ACTUAL NUMBER OF MINOR NEUTRAL SPECIES
C
C       IPLUSH    IONS + MINORS
C
C       IPNP1     IPLUSH + 1
C
C       MAJORS    THE ACTUAL NUMBER OF MAJOR NEUTRAL SPECIES
C
C       NATONS    IPLUSH + MAJORS
C
C       NATNP1    NATONS + 1
C
C       NR        THE ACTUAL NUMBER OF CHEMICAL REACTIONS
C                        (INCLUDING DEPOSITION)
C
C       NDR       THE ACTUAL NUMBER OF REACTIONS INVOLVING DEPOSITION
C
C       NP        THE ACTUAL MAXIMUM NUMBER OF REACTANTS PER REACTION
C
        PARAMETER   MZ     = 151
        PARAMETER   MACTIV =  14
        PARAMETER   MATONS =  20
        PARAMETER   MATNP1 = MATONS + 1
        PARAMETER   MR     =  70
        PARAMETER   MDR    =  25
        PARAMETER   MP     =   3
C
        COMMON / SIZE / NZ, IONS, IONSP1, MINORS, IPLUSH, IPNP1, MAJORS,
     *                  NATONS, NATNP1, NR, NDR, NP
C
C
C***  THE VARIABLES AND VARIOUS OTHER ASSOCIATED ITEMS  ***
C
C   THE CHEMISTRY VARIABLES:
C
C       ASYMBL    A SIX CHARACTER SYMBOL TO IDENTIFY EACH SPECIE
C                        (INCLUDING ELECTRONS)
```

*** MEMBER INITAL OLD DATE = 81.342 TIME = 10:24 CHECKSUM = 2FB41B88

```
305* C
306* C       AM        THE ATOMIC MASS OF EACH SPECIE
307* C
308* C       ASP       THE ATOMIC SPECIES DENSITIES
309* C
310* C       NE        THE ELECTRON DENSITY AT THE OLD AND NEW TIME STEP
311* C
312* C       DMIN      THE MINIMUM VALUE THAT A DENSITY CAN HAVE
313* C                 AT A GRID POINT
314* C
315* C       LB        AN INDEX GIVING THE TYPE OF BOUNDARY CONDITION
316* C                 TO APPLY
317* C
318* C       UB        THE LOCATION OF THE UPPER BOUNDARY FOR EACH SPECIE
319* C                 FOR THE PURPOSES OF THE CONTINUITY EQUATION
320* C
321* C       BV        FOR THE MINOR NEUTRALS, A BOUNDARY VALUE
322* C
323* C       AA        FOR THE MINOR NEUTRALS, A DIFFUSION COEFFICIENT
324* C
325* C       BORDER    THE ORDER IN WHICH THE VARIOUS CONTINUITY EQUATIONS
326* C                 ARE SOLVED -- ALL ION EQUATIONS MUST BE SOLVED
327* C                 BEFORE ANY MINOR NEUTRAL EQUATION
328* C
329*         INTEGER     ASYMBL(6,MATMP1), LB(MACTIV), BORDER(MACTIV)
330*         REAL**      ASP  (MZ,MATOMS), AM(MATOMS), NE(MZ,2), DMIN(MZ)
331*         REAL**      UB(MACTIV),       BV(MACTIV), AA(MACTIV)
332* C
333*         COMMON / CVAR / ASYMBL, AM, ASP, NE, DMIN, LB, UB, BV, AA,
334*        *                BORDER
335* C
336* C   THE HYDRODYNAMIC VARIABLES:
337* C
338* C       TN        THE AMBIENT MAJOR NEUTRAL TEMPERATURE
339* C
340* C       TI        THE ION TEMPERATURE AT THE OLD AND NEW TIME STEP
341* C
342* C       TE        THE ELECTRON TEMPERATURE AT THE OLD AND NEW TIME STEP
343* C
344* C       U         THE MINOR NEUTRAL WIND VELOCITY IN THE X-DIRECTION
345* C
346* C       V         THE MINOR NEUTRAL WIND VELOCITY IN THE Y-DIRECTION
347* C
348* C       EVIB      THE VIBRATIONAL ENERGY OF N2 -- NOT CURRENTLY USED
349* C
350* C       EFDX      THE PRESSURE GRADIENT IN THE X-DIRECTION
351* C
352* C       EFDY      THE PRESSURE GRADIENT IN THE Y-DIRECTION
353* C
354* C       VIN       ION NEUTRAL COLLISION FREQUENCY
355* C
```

*** MEMBER INITAL OLD DATE = 81.342 TIME = 10:24 CHECKSUM = 2FF01888

```
C       MEW       VISCOSITY
C
C       EDYDC     EDDY DIFFUSION COEFFICIENT
C
        REAL*8       TN(MZ), TI(MZ,2), TE(MZ,2)
        REAL*8       U(MZ,2), V(MZ,2), EVIB(MZ)
        REAL*8       DPDX(MZ), DPDY(MZ), VIN(MZ), MEW(MZ),
     *               EDYDC(MZ)
C
        COMMON / HVAP / TN, TI, TE, U, V, EVIB,
     *                  DPDX, DPDY, VIN, MEW, EDYDC
C
C  SOME POINTERS INTO THE ASP ARRAY
C
C       PTH       THE SECOND INDEX FOR ASP WHERE H         BEGINS
C
C       PTHE      THE SECOND INDEX FOR ASP WHERE HE        BEGINS
C
C       PTO       THE SECOND INDEX FOR ASP WHERE O         BEGINS
C
C       PTN2      THE SECOND INDEX FOR ASP WHERE N2        BEGINS
C
C       PTO2      THE SECOND INDEX FOR ASP WHERE O2        BEGINS
C
        INTEGER  PTH, PTHE, PTO, PTN2, PTO2
C
        COMMON / APOINT / PTH, PTHE, PTO, PTN2, PTO2
C
C
C***  THE GRID POINTS AND RELATED VALUES  ***
C
C   THE VARIABLES:
C
C       Z         THE GRID POINTS  ---  ALTITUDE  (IN KM)
C
C       DKDZ      INFORMATION ABOUT GRID SPACING
C
C       RSQ       R**2, WHERE R IS THE RADIAL GEOCENTRIC DISTANCE
C
C       RRSQ      RECIPROCAL OF RSQ
C
        REAL*8       Z(MZ), DKDZ(MZ), RRSQ(MZ), RSQ(MZ)
C
        COMMON / MESHA / Z, DKDZ, RRSQ, RSQ
C
C   THE SCALAR VARIABLES:
C
C       MZM1      MZ-1
C
C       MZ
C
```

*** MEMBER INITAL OLD DATE = 81.342 TIME = 10:24 CHECKSUM = 2F0A1B8B

```
C       DZ1
C
C       DZHZ
C
C       ZTOP
C
C       ZBOT
C
        COMMON / MESHS / NZM1, DZ0, DZ1, DZHZ, ZTOP, ZBOT
C
C
C***  THE CONSTANT COMMON BLOCKS  ***
C
C   THE NUMERICAL CONSTANTS:
C
C       DT        THE TIME STEP (IN SEC)
C
        COMMON / NCON /  DT
C
C   THE PHYSICAL CONSTANTS:
C
C       BOLT      BOLTZMANN'S CONSTANT
C
C       AMU       ATOMIC MASS UNIT  (IN KG)
C
C       BMAG      THE MAGNITUDE OF THE EARTH'S MAGNETIC FIELD
C
C       UNITS     TEMPERATURE UNITS
C
C       RE        RADIUS OF EARTH  (IN KM)
C
C       GZERO     GRAVITATIONAL CONSTANT AT EARTH'S SURFACE
C
        COMMON / PCON /  BOLT, AMU, BMAG, UNITS, RE, GZERO
C
C   THE GEOMETRIC VARIABLES:
C
C       LAT       LATITUDE
C
C       CLAT      COS(LAT)
C
C       SLAT      SIN(LAT)
C
C       DEC       DECLINATION OF THE SUN
C
C       CDEC      COS(DEC)
C
C       SDEC      SIN(DEC)
C
C       DTR       DTR ANGLE
C
```

*** MEMBER INITAL OLD DATE = 81.342 TIME = 10:24 CHECKSUM = 2F881B08

```
458* C       CDPA     COS(DIPA)
459* C
460* C       SDPA     SIN(DIPA)
461* C
462* C       CDR
463* C
464* C       PI180    NUMBER OF RADIANS PER DEGREE  (PI/180)
465* C
466*         REAL*8             LAT
467*         COMMON / GEOM /  LAT, CLAT, SLAT,
468*      *                   DEC, CDEC, SDEC,
469*      *                  DIPA, CDPA, SDPA,
470*      *                   CDR, PI180
471* C
472* C
473* C***  AUXILIARY ARRAYS FOR THE COMPUTATION OF CHEMICAL RATES  ***
474* C
475* C   THE VARIABLES:
476* C
477* C       NCRT     THE NUMBER OF PRODUCTION TERMS IN EACH EQUATION
478* C
479* C       ICRATE   A ARRAY OF POINTERS TO THE PARTICULAR PRODUCTION
480* C                TERMS IN EACH EQUATION
481* C
482* C       NPRT     THE NUMBER OF LOSS TERMS IN EACH EQUATION
483* C
484* C       IPRATE   AN ARRAY OF POINTERS TO THE PARTICULAR LOSS
485* C                TERM IN EACH EQUATION
486* C
487* C       NPT      NPT(K) GIVES THE NUMBER OF REACTIONS WITH AT LEAST
488* C                K  REACTANTS
489* C
490* C       IP       IP(K,J) GIVES THE J-TH REACTANT
491* C                IN THE K-TH REACTION WITH AT LEAST J REACTANTS
492* C
493* C       IP       IP(K,J) GIVES THE K-TH REACTION WITH AT LEAST
494* C                J+1  REACTANTS
495* C
496* C       IFLAW    A FLAG FOR EACH REACTION INDICATING WHICH
497* C                TEMPERATURE DEPENDENT REACTION RATE TO PURSUE
498* C
499* C       RA,RB,RC THREE CONSTANTS TO BE USED IN THE APPROPRIATE
500* C                REACTION LAW
501* C
502*         INTEGER  NCRT(NATMP1), ICRATE(NATMP1,MP),
503*      *           NPRT(NATMP1), IPRATE(NATMP1,MP),
504*      *           NPT(MR), IP(MR,MR), IP(MR,MR), IFLAW(MR)
505*         REAL*8   RA(MR), RB(MR), RC(MR)
506* C
507*         COMMON / CREAR / NCRT, ICRATE, NPRT, IPRATE,
508*      *                    NPT,     IP,   IP,
```

*** MEMBER INITAL PLT DATE = 81,342 TIME = 10:24 CHECKSUM = 2FB41BB8

```
509*       *                    IRLAW,     RA,   RB,     RC
510* C
511* C
512* C***  POINTERS FOR THE O+(2D) REACTIONS
513* C
514* C        LRO2D    THE REACTION WHOSE CHEMISTRY RATE COEFFICIENT IS 1
515* C
516* C        NRO2D    THE NUMBER OF O+(2D) REACTIONS
517* C
518* C        IRO2D    IRO2D(J) GIVES THE J-TH O2D REACTION
519* C
520* C        IRO2D    IRO2D(J) GIVES THE OTHER REACTANT (OTHER THAN O+(2D) )
521* C                 INVOLVED IN THE J-TH O2D REACTION
522* C
523* C
524*          INTEGER  IRO2D(MR), IRO2D(MR)
525* C
526*          COMMON / O2DR / LRO2D, NRO2D, IRO2D, IRO2D
527* C
528* C
529* C***  POINTERS FOR PRINTING  ***
530* C
531* C        NRP      THE NUMBER OF PRODUCTION/LOSS TERMS TO PRINT
532* C
533* C        IRP      AN INTEGER ARRAY GIVING THE INDEX OF EACH
534* C                 PRODUCTION/LOSS TERM TO PRINT
535* C
536* C
537*          INTEGER  IRP(MR)
538* C
539*          COMMON / CHEMRP / NRP, IRP
540* C
541* C
542* C***  STORAGE FOR THE DEPOSITION RATES  ***
543* C
544* C   THE VARIABLES:
545* C
546* C        DEPRAT   THE DEPOSITION RATES AT THE GRID POINTS
547* C
548* C        SCI      THE TOTAL ION PRODUCTION RATE
549* C
550* C        SCE      THE ELECTRON HEATING RATE
551* C
552* C
553*          REAL*8   DEPRAT(MZ,MDC)
554*          REAL*8   SCI(MZ), SCE(MZ)
555* C
556*          COMMON / DEPRM / DEPRAT, SCI, SCE
557* C
558* C***  POINTERS TO VARIOUS TYPES OF DEPOSITION REACTIONS
559* C
```

*** MEMBER INITAL PLC DATE = 81,342 TIME = 10:20 CHECKSUM = 2FB01888

```
560* C
561* C       NRDI     THE NUMBER OF IONIZATION REACTIONS
562* C
563* C       NRDD     THE NUMBER OF DISSOCIATION REACTIONS
564* C
565* C       NRDID    THE NUMBER OF REACTIONS INVOLVING BOTH IONIZATION
566* C                AND DISSOCIATION
567* C
568* C       NRDDUP   THE NUMBER OF REACTIONS INVOLVING DUPLICATES OF
569* C                PREVIOUS PHOTO DEPOSITIONS
570* C
571* C       NRNT     THE NUMBER OF REACTIONS INVOLVING NIGHT TIME
572* C                DEPOSITIONS
573* C
574* C       NRXRAY   THE NUMBER OF REACTIONS INVOLVED IN XRAY PRODUCTION
575* C                OF IONS
576* C
577* C       IRDI     AN INTEGER ARRAY GIVING THE INDEX IN THE ARRAY 'DEPRAT'
578* C                FOR THE IONIZATION RATES
579* C
580* C       IRDD     AN INTEGER ARRAY GIVING THE INDEX IN THE ARRAY 'DEPRAT'
581* C                FOR THE DISSOCIATION RATES
582* C
583* C       IRDID    AN INTEGER ARRAY GIVING THE INDICES FOR DISSOCIATION
584* C                AND IONIZATION
585* C
586* C       IRDDUP   AN INTEGER ARRAY GIVING THE INDICES FOR THE
587* C                DUPLICATES
588* C
589* C       IRNT     AN INTEGER ARRAY GIVING THE INDEX FOR NIGHT TIME
590* C                DEPOSITION REACTIONS
591* C
592* C       IRXRAY   AN INTEGER ARRAY GIVING THE INDICES FOR THE REACTIONS
593* C                INVOLVED IN XRAY PRODUCTION OF IONS
594* C
595* C
596*         INTEGER  IRDI(MDR), IRDD(MDR), IRDID(MDR), IRDDUP(MDR)
597*         INTEGER  IRNT(MDP), IRXRAY(MDP)
598* C
599*         COMMON / SRDEP / NRDI, NRDD, NRDID, NRDDUP, NRNT, NRXRAY,
600*     *                    IRDI, IRDD, IRDID, IRDDUP, IRNT, IRXRAY
601* C
602* C
603* C***  THE MAIN CONTROL PARAMETERS  ***
604* C
605* C
606* C       MAXSTP   THE MAXIMUM NUMBER OF TIME STEPS TO COMPUTE
607* C
608* C       MDMAX    THE MAXIMUM MDLP AND
609* C       IDAY     DAY TO WHICH TO COMPUTE
610* C
```

*** MEMBER INITAL OLD DATE = 81,342 TIME = 10124 CHECKSUM = 2FB41BB8

```
C       ISTEP    THE CURRENT STEP
C
C       HR       THE CURRENT HOUR
C
C       IDAY     THE CURRENT DAY
C
C       DHR      THE TIME STEP IN HOURS
C
C       MAT      THE YEAR FOR THE APPROPRIATE JACCHIA MODEL OF THE
C                        AMBIENT NEUTRAL ATMOSPHERE
C
C       IAMBT    THE NUMBER OF TIME STEPS BETWEEN CALCULATIONS
C                        OF THE AMBIENT NEUTRAL TEMPERATURE
C                        AND THE MAJOR NEUTRAL DENSITIES
C
C       PGSCL    PRESSURE GRADIANT SCALE FACTOR
C
C       IDEP     THE NUMBER OF TIME STEPS BETWEEN CALCULATION OF
C                        THE DEPOSITION RATES
C
C       ICHEM    A LOGICAL VARIABLE:  .TRUE.  IF CHEMISTRY IS DONE
C                                     .FALSE.  IF CHEMISTRY IS NOT DONE
C
C       TRNP     A LOGICAL VARIABLE:  .TRUE.  IF TRANSPORT IS DONE
C                                     .FALSE.   OTHERWISE
C
C       ITR      THE NUMBER OF ITERATIONS IT TOOK TO GET THE ION
C                EQUATIONS TO CONVERGE
C
C       CONVRG   A LOGICAL VARIABLE:  .TRUE.  IF THE IONS CONVERGED
C                                     .FALSE.  IF THEY DID NOT
C
      LOGICAL     ICHEM, TRNP, CONVRG
C
      COMMON / MCTRL / MAXSTP, HRMAX, NDAY,
     *                 ISTEP, HR,    IDAY,
     *                   DHR,
     *                   MAT, IAMBT, PGSCL,
     *                  IDEP, ICHEM,
     *                  TRNP,   ITR, CONVRG
C
C
C*** THE OUTPUT CONTROL VARIABLES ***
C
C   THE PLOTTING CONTROL VARIABLES:
C
C       IPLDAY   THE VALUE IF IDAY WHEN PDSPLAY WAS LAST CALLED
C
C       IPTP
C
C       IZPLT    THE INDEX OF THE ALTITUDE AT WHICH 24-HOUR PLOTS
```

*** MEMBER INITAL OLD DATE = 81,342 TIME = 10:24 CHECKSUM = 2F001808

```
C                 ARE TO BE MADE
C
C       SPDAY     THE NUMBER OF SECONDS PER DAY
C
C       PSYMBL    AN ARRAY OF SYMBOLS TO IDENTIFY A SPECIE ON THE
C                 DENSITY PLOT
C
        REAL*8      PSYMBL(MATMP1)
C
C
        COMMON / PCTRL / IOLDAY, NDTP, SPDAY, NZPLT, PSYMBL
C
C   THE RESTART CONTROL VARIABLES:
C
C       LDUMP
C
C       LTDMP
C
C       DDUMP
C
C       TDUMP
C
        INTEGER    DDUMP, TDUMP
C
        COMMON / DCTRL / LDUMP, LTDMP, DDUMP, TDUMP
C
C
C***  CIFER DECLARATIONS  ***
C
        LOGICAL   LPRIC, NSTART
        INTEGER   BLANK
        REAL *8   MGDPA,KP
C
C--     THIS COMMON BLOCK IS USED BY  "DSPLAY" AND "RSTART"
C
        COMMON / CPLT / NPT, PZ(121,5)
C
C--     THIS COMMON BLOCK IS IN  THE CIFER MACRO  #SCF
C
        COMMON / START /
     *     ZS(50), US(50), VS(50), EVS(50), ASPS(50,MATMS)
C
C--     THIS COMMON BLOCK IS USED BY "JAC71"
C
        COMMON / NOUT / FC0, FC12, FC02, EUVFD
C
C***  INITIALIZING FIXED CONSTANTS  ***
C
        DATA  BLANK / '    '  /
        DATA  PIE   / 3.141593 /, PR180 / 1.745329E-02 /
        DATA  SPDAY / 86400.0  /, SPHR  / 3600.0 /
```

*** MEMBER INITAL OLD DATE = 81.342 TIME = 10:24 CHECKSUM = 2F041008

```
713*          DATA  GZERO / 980.665  /, RE    / 6370.0 /
714*          DATA  OMAG  /   0.25   /
715*          DATA  UNITS / 1.16E+04 /, BOLT / 1.38044E-16 /,
716*     &          AMU   / 1.672521-24 /
717* C
718*          NAMELIST / CNTS / IONS, MINORS, NZ, ZBOT, ZTOP, DZ0, ZPLOT,
719*     &                      DT, PGOPA, LAT, PGRADA, HPHA, PGSCL,
720*     &                     EEMX, FLUXF, JAX1, JAXN
721* C
722*          DATA      ZBOT   / 70.0 /, ZTOP / 10000.0 /
723*          DATA      PGRADA / 10.0 /
724*          DATA      HPHA   /  0.0 /, PGSCL  / 1.0 /
725*          DATA      EEMX   /  1.0 /, FLUXF  / 1.0 /
726*          DATA      JAX1   /  150 /, JAXN   / 50 /
727* C
728*          NAMELIST / CTRL / MAXSTP, HRMAX, NDAY, IAMBT, IDEP, ICHEM,
729*     &                      TRNP, LINCP, LOTCP, LPRIC, NSTART,
730*     &                      LDUMP, LTDMP, TDUMP, QDUMP
731* C
732*          DATA      IAMBT  /     2   /, IDEP   /     2  /
733*          DATA      ICHEM  / .TRUE.  /, TRNP   / .TRUE. /
734*          DATA      LPRIC  / .TRUE.  /
735*          DATA      LINCR  /     5   /, LOTCR  /     6 /
736*          DATA      NSTART / .FALSE. /
737* C
738*          NAMELIST/SOLARP/FBAR, F, DAY, KP, TNOT, MAT,
739*     *                    FC0, FCN2, FC02, FUVFD
740* C
741*          EXTERNAL   JAC65, JAC71
742*          EXTERNAL   RTC00
743* C
744* C***  INITIALISE ERROR ROUTINES  ***
745* C
746*          CALL COMMON
747* C
748* C*** INITIALISE ATMOSPHERIC ROUTINE ***
749* C
750*          READ (5,SOLARP)
751*          WRITE(6,SOLARP)
752*          IF(MAT .EQ. 1965)CALL IJAC65(FBAR, F, DAY, KP, TNOT, .TRUE.)
753*          IF(MAT .EQ. 1971)CALL IJAC71(FBAR, F, DAY, KP, TNOT, .TRUE.)
754* C
755* C***  READ SOME CONTROL VARIABLES  ***
756* C
757*          READ(5,CTRL)
758*          WRITE(6,CTRL)
759* C
760* C***  READ SOME NUMERICAL AND PHYSICAL CONSTANTS  ***
761* C
762*          READ(5,CNTS)
763*          WRITE(6,CNTS)
```

*** MEMBER INITAL PLF DATE = 81,342 TIME = 10:24 CHECKSUM = 2F841888

```
764*          MAJORS = 5
765*          IONSP1 = IONS   + 1
766*          IPLUSM = IONS   + MINORS
767*          IPMP1  = IPLUSM + 1
768*          NATOMS = IPLUSM + MAJORS
769*          NATMP1 = NATOMS + 1
770* C
771* C***  CHECK FOR UNDERDIMENSIONED ARRAYS ***
772* C
773*          IF(NATOMS .GT. MATOMS) GO TO 1000
774*          IF(MZ     .GT. MZ    ) GO TO 1010
775* C
776* C***  READ INFORMATION ABOUT THE ATOMIC VARIABLES  ***
777* C
778*          DO 3 J=1,NATMP1
779*            DO 3 I=1,6
780*     3        ASYMBL(I,J) = BLANK
781* C
782*          DO 5 J=1,IPLUSM
783*            READ(5, 9) (ASYMBL(I,J),I=1,6), AM(J), LB(J),
784*     *                  UB(J), BV(J), AA(J), PSYMBL(J)
785*     5    CONTINUE
786*     9    FORMAT(6A1,F8.1,I3,3F8.1,3X,A1)
787*          DO 10 J=IPMP1,NATOMS
788*            READ(5,12) (ASYMBL(I,J),I=1,6), AM(J), PSYMBL(J)
789*    10    CONTINUE
790*    12    FORMAT(6A1,F8.1,27X,A1)
791*          READ(5,18) (ASYMBL(I,NATMP1),I=1,6), PSYMBL(NATMP1)
792*    18    FORMAT(6A1,35X,A1)
793*          READ(5,20) (RORDER(J),J=1,IPLUSM)
794*    20    FORMAT(2013)
795* C
796* C***  CHECK THE RORDER ARRAY ***
797* C
798*          DO 30 J=1,IONS
799*            IF(RORDER(J) .LT. 1  .OR.  RORDER(J) .GT. IONS) GO TO 1100
800*            IF(J .EQ. 1) GO TO 30
801*            JM1 = J - 1
802*            DO 25 JJ=1,JM1
803*              IF(RORDER(J) .EQ. RORDER(JJ)) GO TO 1100
804*    25      CONTINUE
805*    30    CONTINUE
806*          DO 40 J=IONSP1,IPLUSM
807*            IF(RORDER(J) .LT. IONSP1  .OR.  RORDER(J) .GT. IPLUSM)
808*     *                  GO TO 1100
809*            IF(J .EQ. IONSP1) GO TO 40
810*            JM1 = J - 1
811*            DO 35 JJ=IONSP1,JM1
812*              IF(RORDER(J) .EQ. RORDER(JJ)) GO TO 1100
813*    35      CONTINUE
814*    40    CONTINUE
```

*** PEPPER INITAL OLD DATE = 81,342 TIME = 10:24 CHECKSUM = 2FB01BB8

```
C
C*** INITIALIZE POINTERS TO THE MAJOR NEUTRALS IN THE ASP ARRAY ***
C
      PTH  = IPLUSH + 1
      PTHE = PTH    + 1
      PTO  = PTHE   + 1
      PTN2 = PTO    + 1
      PTO2 = PTN2   + 1
C
C*** READ INITAL DENSITY PROFILES FROM DATA CARDS ***
C
      L = 0
   60   L = L + 1
        IF(L .GT. 50)GO TO 100
        READ 70, ZS(L), US(L), VS(L), EVS(L)
   70   FORMAT(F8.1,7E8.1)
        IF(ZS(L) .LE. 0.0)GO TO 100
        READ 80, (ASPS(L,J),J=1,IONS)
        READ 80, (ASPS(L,J),J=IONSP1,IPLUSH)
   80   FORMAT(8X,7E8.1)
        GO TO 60
  100   LMAX = L - 1
C
C*** GENERATE THE MESH ***
C
      NZM1 = NZ - 1
      CALL ZMESH
      PRINT 120
  120 FORMAT('1    STUFF FROM -INITAL-',//,9X,'I',9X,'Z',8X,'DZ',
     1   6X,'EDDY')
C
C*** GENERATE THE INITIAL CONDITIONS PLUS OTHER ITEMS ***
C
      HAV  = 6.0
      HKK  = 2.0*HAV
      ZNOT = 100.0
      IF(DAT .EQ. 1971) EDDY0 = 1.0E6
      IF(DAT .EQ. 1965) EDDY0 = 0.5E6
      DZMN = 1.0E+50
      DO 500 I = 1,NZ
        RSQ(I)   = (RE + Z(I))**2
        RSQ1(I)  = 1.0/RSQ(I)
        EDYDC(I) = EDDY0
        IF(Z(I) .LT. ZNOT) EDYDC(I) = EDDY0*EXP((Z(I) - ZNOT)/HKK)
C
        RESID = ABS(Z(I) - ZPLOT)
        IF(RESID .GT. DZMN) GO TO 125
          IZPLT = I
          DZMN = RESID
C
  125   DO 150 L = 2,LMAX
```

*** MEMBER INITAL ALT DATE = 81.342 TIME = 10:20 CHECKSUM = 2F881BB8

```
A66*                IS = L - 1
A67*                IF(ZS(L) .GE. Z(I))GO TO 200
A68*   150        CONTINUE
A69*   200        RAT    = (Z(I) - ZS(LS))/(ZS(LS+1) - ZS(LS))
A70*              U(I,2)    = US(LS) + RAT*(US(LS+1) - US(LS))
A71*              V(I,2)    = VS(LS) + RAT*(VS(LS+1) - VS(LS))
A72*              U(I,1)    = U(I,2)
A73*              V(I,1)    = V(I,2)
A74*              EVIP(I)   = EVS (LS)*(EVS (LS+1)/EVS (LS))**RAT
A75* C
A76*              DO 225 J=1,IPLUSH
A77*                ASP(I,J) = ASPS(LS,J) * (ASPS(LS+1,J)/ASPS(LS,J))**RAT
A78*   225        CONTINUE
A79*              DO 250 J=IPMP1,NATOMS.
A80*   250          ASP(I,J) = 0.0
A81* C
A82*              TE(I,2) = 0.0
A83*              TI(I,2) = 0.0
A84*              NE(I,2) = 0.0
A85*              DO 275 J=1,IONS
A86*   275          NE(I,2) = NE(I,2) + ASP(I,J)
A87*              TE(I,1) = TE(I,2)
A88*              TI(I,1) = TI(I,2)
A89*              NE(I,1) = NE(I,2)
A90* C
A91*              SOE(I) = 0.0
A92*              SOI(I) = 0.0
A93*              DO 300 J=1,MDR
A94*                EPPRAT(I,J) = 0.0
A95*   300        CONTINUE
A96*              DELTZ = 1.0E-05/DKDZ(I)
A97* C
A98*              PRINT 400, I, Z(I), DELTZ, EDYDC(I)
A99*   400        FORMAT(5X,I5,1P12(10.3)
A00*   500    CONTINUE
A01* C
A02* C***  INITIALIZE OUTPUT ROUTINE  ***
A03* C
A04*           CALL OSPLI
A05* C
A06* C***  CALCULATE THE GEOMETRIC VARIABLES  ***
A07* C
A08*           DEC  = 23.5*SIN(2.0*PIE*(DAY - 80.0)/365.0)
A09*           CDEC = COS(P0180*DEC)
A10*           SDEC = SIN(P0180*DEC)
A11*           CLAT = COS(P0180*LAT)
A12*           SLAT = SIN(P0180*LAT)
A13*           CCC  = 0.5*PIE/SPDAY*SLAT
A14*           DIPA = P0180*HGDPA
A15*           SDPA = SIN(DIPA)
A16*           CDPA = COS(DIPA)
```

*** MEMBER INITAL PLD DATE = 81.342 TIME = 10:24 CHECKSUM = 2F841888

```
C
            IF(.NOT. ICHEM) GO TO 600
C
C***  INITIALIZE CHEMISTRY ROUTINE  ***
C
            IPRIC = 0
            IF(LPRIC) IPRIC = 1
            CALL IAPTP(0,0,0,0,IPRIC)
            CALL APTP(CTCON, ASYMPL, 6, MATPP1, IPLUSM, MAJORS+1,
     *                ICRATE, NCRT, IDRATE, NDRT, IU, IP, NPT, NR,
     *                NB, NB)
            NF = NPT(1)
            IF(LOOP2D .LT. 1) GO TO 540
            IF(LOOP2D .LT. 1  .OR.  LOOP2D .GT. NR) GO TO 1200
   540      IF(LPRIC) CALL RTCSPO
C
            CALL VSAINF(0.0, 0.0E-03, NR+MAJORS+1, 0.0, 0.0, -1.0E+03)
C
C*** INITIALISE DEPOSITION ROUTINE ***
C
            CALL DEPINT(FLUXF, CEMX, RE+ZTOP+1.0, RE+ZBOT-1.0, 1.0E-03,
     *                      JAX1, JAXN,   LPRIC,        LINCR)
C
   600      CONTINUE
C
C*** INITIALISE PRESSURE GRADIENT ROUTINE ***
C
            CALL PGRADI(PGRADA, KPHA)
C
C*** INITIALISE TIME LOOP ***
C
            IDAY = 1
            ISTEP = 0
            HF   = 0.0
            DTR = DT/SPHR
            ITR = 0
            CONVRG = .TRUE.
            NSTP = IFIX(SPDAY/(DT*120.0) + .999999)
C
C***  DECIDE ON A RESTART  ***
C
            IF(.NOT.RSTART) RETURN
            DTSAV = DT
            CALL RSTART(LUNMP,LTRMP)
            IF(ABS(DTSAV - DT)/DT .LT. 1.0E-04)GO TO 850
            PRINT 800, DTSAV, DT
   800      FORMAT(/,5X,'CHANGE OF TIME STEP ON RESTART,  DTNEW, DTOLD = ',
     1      1P2E10.3,' SEC.')
            TIME = DT*FLOAT(ISTEP)
            DT = DTSAV
            DTR = DT/SPHR
```

*** MEMBER INITAL OLD DATE = 81,342 TIME = 10:24 CHECKSUM = 2FB41B08

```
      268*          ISTEP = IFIX(TIME/DT + .05)
      269*    850   NSTP = IFIX((IDAY*SPDAY - TIME)/(DT*MAX0(1, 120 - NPT))
      270*     *                + .999999)
      271*          IPLDAY = IDAY
      272* C
      273*          RETURN
      274* C
      275* C***  ERROR MESSAGES  ***
      276* C
      277*  1000    MPPP = NATOMS
      278*          PRINT 1001, NATOMS, MPPP
      279*  1001    FORMAT(' INSUFFICIENT STORAGE FOR ATOMIC VARIABLES'/
      280*     *           ' YOU REQUESTED NATOMS = ',I3,' WHEN NATOMS = ',I3)
      281*          STOP
      282* C
      283*  1010    MPPP = NZ
      284*          PRINT 1011, NZ, MPPP
      285*  1011    FORMAT(' INSUFFICIENT STORAGE FOR MESH DEPENDENT VARIABLES'/
      286*     *           ' YOU REQUESTED NZ     = ',I3,' WHEN MZ     = ',I3)
      287*          STOP
      288* C
      289*  1100    PRINT 1101, (RORDER(L), L=1,IPLUSM)
      290*  1101    FORMAT(' RORDER IS NOT AN ACCEPTABLE PERMUTATION'/
      291*     *           ' RORDER = ',20I3)
      292*          STOP
      293* C
      294*  1200    PRINT 1201
      295*  1201    FORMAT(5(/), ' RTCON WAS UNABLE TO FIND AN O+(2D) REACTION',
      296*     *                 ' WHOSE CHEMISTRY RATE WAS EQUAL TO 1')
      297*          STOP
      298* C
      299*          END
```

*** MEMBER INITAL COPIED -- 999 RECORDS, DATE = 81,342 TIME = 10:24 CHECKSUM = 2FB41BF8

*** MEMBER RICRN CLE DATE = 81,342 TIME = 10:20 CHECKSUM = 1F228528

```
  1*          SUBROUTINE  RICRN(REACT, SYMB, NCPS, MSY, FRN, LRN, IRT)
  2* C         ----------  -----
  3* C
  4* C
  5* C   READ THE REACTION RATE CONSTANTS ASSOCIATED WITH THE CURRENT
  6* C       REACTION BEING DECODED BY "RARTR"
  7* C       ALL THE DEPOSITION REACTIONS MUST BE PLACED AT THE END OF THE
  8* C       LIST OF REACTIONS
  9* C
 10* C   FOR EACH REACTION THE INPUT IS AS FOLLOWS
 11* C
 12* C       1)  A CONTROL CARD CONSISTING OF SEVERAL FOUR-CHARACTER SYMBOLS
 13* C               INDICATING THE TYPE OF REACTION
 14* C
 15* C                   A)  THE FIRST SYMBOL IS 'CHEM' TO INDICATE REACTIONS
 16* C                       INVOLVING CHEMISTRY
 17* C
 18* C                   B)  THE SECOND SYMBOL IS 'DEPO' TO INDICATE REACTIONS
 19* C                       INVOLVING PHOTO DEPOSITION
 20* C
 21* C                   C)  FOR PHOTO-DEPOSITION REACTIONS THE THIRD SYMBOL IS
 22* C                           'I   ' FOR IONIZATION
 23* C                           'D   ' FOR DISSOCIATION
 24* C                           'ID  ' FOR IONIZATION AND DISSOCIATION
 25* C                           'DUP ' FOR A DUPLICATION OF THE PREVIOUS
 26* C                                  REACTION
 27* C
 28* C                   D)  THE FOURTH SYMBOL IS 'OP2D' FOR REACTIONS
 29* C                       WITH O+(2D) AS AN INTERMEDIATE PRODUCT
 30* C
 31* C                   E)  THE FIFTH SYMBOL IS 'INT ' TO INDICATE THAT
 32* C                       THE DEPOSITION REACTION IS IMPORTANT AT
 33* C                       NIGHT TIME
 34* C
 35* C                   F)  THE SIXTH SYMBOL IS 'XRAY' FOR THE TWO DEPOSITION
 36* C                       REACTIONS INVOLVED IN THE XRAY PRODUCTION
 37* C                       OF O+ AND O2+
 38* C
 39* C                   G)  THE SEVENTH SYMBOL IS 'PRIN' IF THE PRODUCTION/LOSS
 40* C                       RATE CORRESPONDING TO THIS REACTION IS TO BE
 41* C                       PRINTED
 42* C
 43* C
 44* C       2)  FOR REACTIONS INVOLVING CHEMISTRY THE NEXT CARD CONTAINS
 45* C               DATA ASSOCIATED WITH THE CHEMICAL REACTION
 46* C
 47* C               A) THE FIRST NUMBER IS AN INTEGER GIVING THE
 48* C                   APPROPRIATE REACTION LAW
 49* C
 50* C               B)  THE NEXT THREE NUMBERS ARE THREE CONSTANTS TO
 51* C                   BE USED BY "CCATA" TO CONSTRUCT THE
```

*** MEMBER DICOM OLD DATE = 81.342 TIME = 10:24 CHECKSUM = 1F228528

```
C                          APPROPRIATE REACTION RATE
C
C
C
C
C*** THE PROGRAM SIZE ***
C
C   THE PARAMETERS:
C
C       MZ        THE MAXIMUM NUMBER OF GRID POINTS
C
C       MACTIV    THE MAXIMUM NUMBER OF ACTIVE SPECIES
C                         (IONS PLUS MINOR NEUTRALS)
C
C       MATOMS    THE MAXIMUM NUMBER OF SPECIES
C                         (NOT COUNTING ELECTRONS)
C
C       MR        THE MAXIMUM NUMBER OF CHEMICAL REACTIONS
C                         (INCLUDING DEPOSITION)
C
C       MDR       THE MAXIMUM NUMBER OF REACTIONS INVOLVING DEPOSITION
C
C       MP        THE MAXIMUM NUMBER OF REACTANTS PER REACTION
C
C   THE VARIABLES:
C
C       NZ        THE ACTUAL NUMBER OF GRID POINTS USED
C
C       IONS      THE ACTUAL NUMBER OF IONS
C
C       IONSP1    IONS  + 1
C
C       MINORS    THE ACTUAL NUMBER OF MINOR NEUTRAL SPECIES
C
C       IPLUSM    IONS + MINORS
C
C       IPMP1     IPLUSM + 1
C
C       MAJORS    THE ACTUAL NUMBER OF MAJOR NEUTRAL SPECIES
C
C       NATOMS    IPLUSM + MAJORS
C
C       NATMP1    NATOMS + 1
C
C       NR        THE ACTUAL NUMBER OF CHEMICAL REACTIONS
C                         (INCLUDING DEPOSITION)
C
C       NDR       THE ACTUAL NUMBER OF REACTIONS INVOLVING DEPOSITION
C
C       NP        THE ACTUAL MAXIMUM NUMBER OF REACTANTS PER REACTION
C
```

*** MEMBER DICON OLD DATE = 81,342 TIME = 10:20 CHECKSUM = 1E228528

```
103*          PARAMETER   PZ     = 151
104*          PARAMETER   MACTIV =  14
105*          PARAMETER   MATOMS =  20
106*          PARAMETER   MATMP1 = MATOMS + 1
107*          PARAMETER   MR     =  70
108*          PARAMETER   MDR    =  25
109*          PARAMETER   MM     =   3
110* C
111*          COMMON / SIZE / PZ, IONS, IONSP1, NIRORS, IPLUSM, IPMP1, MAJORS,
112*         *                MATOMS, MATMP1, MR, MDR, MM
113* C
114* C
115* C***  AUXILIARY ARRAYS FOR THE COMPUTATION OF CHEMICAL RATES  ***
116* C
117* C   THE VARIABLES:
118* C
119* C       NCRT     THE NUMBER OF PRODUCTION TERMS IN EACH EQUATION
120* C
121* C       ICRATE   A ARRAY OF POINTERS TO THE PARTICULAR PRODUCTION
122* C                TERMS IN EACH EQUATION
123* C
124* C       NLRT     THE NUMBER OF LOSS TERMS IN EACH EQUATION
125* C
126* C       ILRATE   AN ARRAY OF POINTERS TO THE PARTICULAR LOSS
127* C                TERM IN EACH EQUATION
128* C
129* C       NRT      NRT(K) GIVES THE NUMBER OF REACTIONS WITH AT LEAST
130* C                K  REACTANTS
131* C
132* C       IR       IR(K,J) GIVES THE J-TH REACTANT
133* C                IN THE K-TH REACTION WITH AT LEAST J REACTANTS
134* C
135* C       IP       IP(K,J) GIVES THE K-TH REACTION WITH AT LEAST
136* C                J+1  REACTANTS
137* C
138* C       IFLAM    A FLAG FOR EACH REACTION INDICATING WHICH
139* C                TEMPERATURE DEPENDENT REACTION RATE TO PURSUE
140* C
141* C       RA,RB,RC THREE CONSTANTS TO BE USED IN THE APPROPRIATE
142* C                REACTION LAW
143* C
144*          INTEGER  NCRT(MATMP1), ICRATE(MATMP1,MM),
145*         *         NLRT(MATMP1), ILRATE(MATMP1,MM),
146*         *         NRT(MM), IR(MR,MM), IP(MR,MM), IFLAM(MM)
147*          REAL*8   RA(MM), RB(MM), RC(MM)
148* C
149*          COMMON / CHEMM / NCRT, ICRATE, NLRT, ILRATE,
150*         *                  NRT,     IR,   IP,
151*         *                IFLAM,     RA,   RB,     RC
152* C
```

*** MEMBER DICON CLC DATE = 81.342 TIME = 10:20 CHECKSUM = 1E228528

```
C***  POINTERS FOR THE O+(2D) REACTIONS
C
C       LROP2D   THE REACTION WHOSE CHEMISTRY RATE COEFFICIENT IS 1
C
C       NROP2D   THE NUMBER OF O+(2D) REACTIONS
C
C       IROP2D   IROP2D(J) GIVES THE J-TH OP2D REACTION
C
C       IROP2D   IROP2D(J) GIVES THE OTHER REACTANT (OTHER THAN O+(2D) )
C                INVOLVED IN THE J-TH OP2D REACTION
C
C
        INTEGER  IROP2D(MR), IBOP2D(MR)
C
        COMMON / OP2DR / LROP2D, NROP2D, IROP2D, IBOP2D
C
C
C***  POINTERS FOR PRINTING  ***
C
C       NPP      THE NUMBER OF PRODUCTION/LOSS TERMS TO PRINT
C
C       IPP      AN INTEGER ARRAY GIVING THE INDEX OF EACH
C                PRODUCTION/LOSS TERM TO PRINT
C
C
C
        INTEGER  IRP(MR)
C
        COMMON / CHEMPR / NRP, IRP
C
C
C***  STORAGE FOR THE DEPOSITION RATES  ***
C
C   THE VARIABLES:
C
C       DEPRAT   THE DEPOSITION RATES AT THE GRID POINTS
C
C       SQI      THE TOTAL ION PRODUCTION RATE
C
C       SQE      THE ELECTRON HEATING RATE
C
C
        REAL**   DEPRAT(NZ,MSP)
        REAL**   SQI(NZ), SQE(NZ)
C
        COMMON / DEPSR / DEPRAT, SQI, SQE
C
C***  POINTERS TO VARIOUS TYPES OF DEPOSITION REACTIONS
C
C
C       NEQI     THE NUMBER OF IONIZATION REACTIONS
C
```

*** MEMBER RTCOM OLD DATE = 81.342 TIME = 10:24 CHECKSUM = 1F228528

```
C       NDDD     THE NUMBER OF DISSOCIATION REACTIONS
C
C       NDDID    THE NUMBER OF REACTIONS INVOLVING BOTH IONIZATION
C                AND DISSOCIATION
C
C       NDDDUP   THE NUMBER OF REACTIONS INVOLVING DUPLICATES OF
C                PREVIOUS PHOTO DEPOSITIONS
C
C       NDNT     THE NUMBER OF REACTIONS INVOLVING NIGHT TIME
C                DEPOSITIONS
C
C       NDXRAY   THE NUMBER OF REACTIONS INVOLVED IN XRAY PRODUCTION
C                OF IONS
C
C       IDDI     AN INTEGER ARRAY GIVING THE INDEX IN THE ARRAY 'DEPRAT'
C                FOR THE IONIZATION RATES
C
C       IDDD     AN INTEGER ARRAY GIVING THE INDEX IN THE ARRAY 'DEPRAT'
C                FOR THE DISSOCIATION RATES
C
C       IDDID    AN INTEGER ARRAY GIVING THE INDICES FOR DISSOCIATION
C                AND IONIZATION
C
C       IDDDUP   AN INTEGER ARRAY GIVING THE INDICES FOR THE
C                DUPLICATES
C
C       IDNT     AN INTEGER ARRAY GIVING THE INDEX FOR NIGHT TIME
C                DEPOSITION REACTIONS
C
C       IDXRAY   AN INTEGER ARRAY GIVING THE INDICES FOR THE REACTIONS
C                INVOLVED IN XRAY PRODUCTION OF IONS
C
C
      INTEGER  IDDI(MDR), IDDD(MDR), IDDID(MDR), IDDDUP(MDR)
      INTEGER  IDNT(MDR), IDXRAY(MDR)
C
      COMMON / SDDEP / NDDI, NDDD, NDDID, NDDDUP, NDNT, NDXRAY,
     *                 IDDI, IDDD, IDDID, IDDDUP, IDNT, IDXRAY
C
C
C***  LOCAL DECLARATIONS  ***
C
      INTEGER   REACT(80), SYMB(NDPS,NSY), PRN(1), LPN(1)
      INTEGER   TEST(20)
      INTEGER   DEPAT, CURNT
      INTEGER   IONIZ, IADD, DISSC, DUPLC
      INTEGER   DEDAT, NIGHT, XRAYT
      INTEGER   PRINT
C
      LOGICAL   DPONLY, NIGHT
C
```

*** MEMBER RICON OLD DATE = 81,342 TIME = 10:20 CHECKSUM = 1F228528

```
256*          DATA      REPRT / 'REPR' /,  CHEMT / 'CHEM' /
257*          DATA      IONIZ / 'I   ' /,  IANDD / 'ID  ' /,
258*     *              DISSC / 'D   ' /,  DUPLC / 'DUP ' /
259*          DATA      OP2DT / 'OP2D' /,  PRPRT / 'PRT ' /
260*          DATA      XRAYT / 'XRAY' /
261*          DATA      PRINT / 'PRIN' /
262* C
263* C***  CHECK FOR FIRST CALL
264* C
265*          IF(IRT .NE. 0) GO TO 50
266*            NCR = 0
267*            NCP = 0
268*            NDDI  = 0
269*            NDDD  = 0
270*            NDDID = 0
271*            NDDDUP = 0
272*            NPRT  = 0
273*            NDXRAY = 0
274*            NDOP2D = 0
275*            LDOP2D = 0
276*            NDP    = 0
277*            DEBUG = .FALSE.
278*            RETURN
279* C
280* C***  READ THE CONTROL LINE FOR THE REACTION
281* C
282*     50   READ(5,110) (TEST(I),I=1,20)
283*    110   FORMAT(20A4)
284*          PRONLY = .FALSE.
285* C
286* C***  IS THIS REACTION TO BE PRINTED  ***
287* C
288*          IF(TEST(7) .NE. PRINT) GO TO 120
289*            NPP = NPP + 1
290*            IPP(NPP) = IRT
291*    120   CONTINUE
292* C
293* C***  DOES THIS REACTION INVOLVE CHEMISTRY
294* C
295*          IF(TEST(1) .NE. CHEMT) GO TO 200
296* C
297* C***  A REACTION INVOLVING CHEMISTRY
298* C
299*          NCR = NCP + 1
300* C
301* C***  READ THE CHEMICAL REACTION RATE COEFFICIENTS
302* C
303*          READ(5,160) IRLAW(IRT), RA(IRT), RB(IRT), RC(IRT)
304*    160   FORMAT(I10,3E10.2)
305*          GO TO 250
306* C
```

*** MEMBER PICON OLD DATE = 81.342 TIME = 10:24 CHECKSUM = 1F228528

```
C*** A REACTION WITHOUT CHEMISTRY (DEPOSITION ONLY)
C
  200   IPLAN(IRT) = 0
        PA   (IRT) = 1.0
        PB   (IRT) = 0.0
        PC   (IRT) = 0.0
        PPOPLY     = .TRUE.
C
C*** WRITE OUT THE CHEMISTRY RATE COEFFICIENTS
C
  250   IF(MOD(IRT,60) .EQ. 1) WRITE(6,260)
  260   FORMAT('1  #   LAW ',9X,'A',9X,'B',9X,'C',10X,
     *         'REACTANTS ------> RESULTS',/)
        WRITE(6,300) IRT, IPLAN(IRT), PA(IRT), PB(IRT), PC(IRT),
     *               (REACT(J),J=1,60)
  300   FORMAT(1X,I3,3X,I3,1X,3E10.2,2X,60A1)
C
C*** DOES THE REACTION INVOLVE DEPOSITION
C
        IF(TEST(2) .EQ. DEPOT) GO TO 400
        IF(PPOPLY)             GO TO 2000
        IF(DEPOT)              GO TO 3000
        RETURN
C
C*** A REACTION INVOLVING DEPOSITION
C
  400   NDR = NDR + 1
        IF(NDR .GT. MDR) GO TO 5000
C
C*** FIND OUT WHAT KIND OF REACTION IT IS
C
        IF(TEST(3) .EQ. IONIZ) GO TO 410
        IF(TEST(3) .EQ. IAUGD) GO TO 430
        IF(TEST(3) .EQ. DISSC) GO TO 420
        IF(TEST(3) .EQ. DUPLC) GO TO 400
C
C*** BE REACH HERE IF THERE IS AN ERROR
C
        GO TO 1000
C
C*** IONIZATION
C
  410   NDI = NDI + 1
        IDI(NDI) = NDR
        GO TO 500
C
C*** DISSOCIATION
C
  420   NDC = NDC + 1
        IDC(NDC) = NDR
        GO TO 500
```

*** MEMBER PICON OLD DATE = 81.342 TIME = 10:20 CHECKSUM = 1E228528

```
C
C*** IONIZATION AND DISSOCIATION
C
  830   NRDID = NRDID + 1
        IRDID(NRDID) = NDR
        GO TO 500
C
C*** DUPLICATE
C
  840   IF(.NOT. DEPSN) GO TO 4000
        NRDDUP = NRDDUP + 1
        IRDDUP(NRDDUP) = NDR
C
  500   CONTINUE
        DEPSN = .TRUE.
C
C*** LOCATE SOME SPECIAL DEPOSITION REACTIONS
C
C
C*** CHECK FOR OP2D REACTIONS
C
C       IT IS ASSUMED THAT THERE IS ONLY ONE SPECIE REACTING WITH
C       O+(2D) IN THE CURRENT REACTION AND THAT REACTANT IS THE
C       SECOND ONE NAMED IN THE REACTION ( THE FIRST BEING O)
C
        IF(TEST(4) .NE. OP2DT) GO TO 720
        NROP2D = NROP2D + 1
        IROP2D(NROP2D) = IRT
        IROP2D(LROP2D) = LPR(2)
        IF(IPLAN(IPT) .EQ. 0 .AND. RA(IRT) .EQ. 1.0) LROP2D = IRT
  720   CONTINUE
C
C*** FIND THE REACTIONS INVOLVED IN THE NIGHTIME DEPOSITION
C
        IF(TEST(5) .NE. NTDPT) GO TO 740
        NPNT = IPNT + 1
        IPNT(IPNT) = NDR
  740   CONTINUE
C
C*** CHECK FOR XRAY PRODUCTION
C
        IF(TEST(6) .NE. XPAYT) GO TO 760
        NRXRAY = NRXRAY + 1
        IRXRAY(NRXRAY) = NDR
  760   CONTINUE
C
        RETURN
C
C
C
        ENTRY PICSPO
```

*** MEMBER PTCON OLD DATE = 81,342 TIME = 10:24 CHECKSUM = 1F228528

```
C       -----  ------
C
C   PRINT SOME ITEMS OF INTEREST THAT DID NOT GET PRINTED BY "ARTP"
C
C
      IF(LRDP2D .LT. 1) GO TO 990
      WRITE(6, 910) LRDP2D
  910 FORMAT( 5(/), ' LRDP2D = ',I5)
      WRITE(6, 920)
  920 FORMAT(//, ' REACTIONS WITH O+(2D) AS AN INTERMEDIATE',
     *           ' PRODUCT-REACTANT' //
     *           '      #   NON-(O) REACTANT'/)
      DO 940 I=1,LRDP2D
        WRITE(6,930) IRDP2D(I), IBDP2D(I)
  930   FORMAT(2I6)
  940 CONTINUE
C
  990 CONTINUE
      RETURN
C
C
C
C***  ERROR MESSAGES
C
 1000 PRINT 1001, IRT, NDE
 1001 FORMAT(5(/),' REACTION #',I3,', DEPOSITION REACTION #',I3,
     *           ' WAS NOT GIVEN A TYPE  (3RD SYMBOL ON CONTROL'
     *           ' CARD)')
      STOP
C
 2000 PRINT 2001, IRT
 2001 FORMAT(5(/),' REACTION #',I3,' WAS NOT IDENTIFIED AS EITHER',
     *           ' CHEMISTRY OR DEPOSITION')
      STOP
C
 3000 PRINT 3001, IRT
 3001 FORMAT(5(/),' REACTION #',I3,' WAS IDENTIFIED AS CHEMISTRY',
     *           ' ONLY WHEN A PREVIOUS DEPOSITION REACTION WAS',
     *           ' ENCOUNTERED'
     *         /  ' ALL PHOTO REACTIONS MUST BE AT THE END OF THE',
     *           ' REACTION LIST')
      STOP
C
 4000 PRINT 4001, IRT
 4001 FORMAT(5(/),' REACTION #',I3,' WAS LABELED A DUPLICATE',
     *           ' PHOTO REACTION WHEN NO PREVIOUS PHOTO REACTION',
     *         /  ' HAD BEEN ENCOUNTERED')
      STOP
C
 5000 PRINT = NDE
      PRINT 5001, NDE, PDRP
```

```
*** MEMBER RICON      OLD DATE = 81,342   TIME = 10:24   CHECKSUM = 1E228528

          460*  5901   FORMAT(' INSUFFICIENT STORAGE FOR THE DEPOSITION ROUTINE'/
          461*      *          ' YOU REQUESTED NDR    = ',I3,' WHEN NDR    = ',I3)
          462*        STOP
          463* C
          464*        END

*** MEMBER RICON    COPIED              --   464 RECORDS,      DATE = 81,342   TIME = 10:24   CHECKSUM = 1E228528
```


DA
FILM